AD NUMBER

AD902068

LIMITATION CHANGES

TO:

Approved for public release; distribution is unlimited.

FROM:

Distribution authorized to U.S. Gov't. agencies only; Test and Evaluation; AUG 1971. Other requests shall be referred to Naval Ship Research and Development Center, Bethesda, MD.

AUTHORITY

USNSRDC ltr 24 Apr 1974

DETERMINATION OF THE (IDEAL PRACTICAL) HOVER EFFICIENCY OF CIRCULATION CONTROL ROTORS

by

Robert M. Williams and Rodney A. Hemmerly

Technical Note AL-212

August 1971

NAVAL SHIP RESEARCH AND DEVELOPMENT CENTER

BETHESDA
MARYLAND
20034

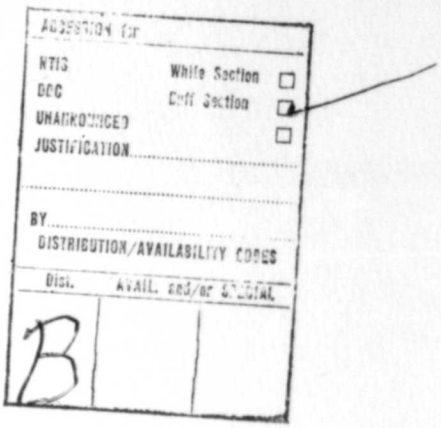
Accession for
NTIS White Section
DDC Buff Section
UNANNOUNCED
JUSTIFICATION
BY
DISTRIBUTION/AVAILABILITY CODES
Dist. AVAIL. and/or SPECIAL
B

(6) DETERMINATION OF THE (IDEAL PRACTICAL) HOVER EFFICIENCY OF CIRCULATION CONTROL ROTORS,

by

(10) Robert M. Williams

[redacted]

Rodney A. Hemmerly

Work performed under sponsorship of the Office of Naval Research, Aeronautics, Code 461, under Project Order #1-0140, NR212-204.

(16) NR-212-204, ONR-PO-1-0140

(11) Aug[redacted]971 (12) 51p. (9) Technical Note AL-212 (14)

TABLE OF CONTENTS

LIST OF FIGURES

LIST OF FIGURES (Concluded)

LIST OF SYMBOLS

c	blade chord, ft
C_{d_e}	section equivalent drag coefficient, (Equation 2)
C_{d_p}	profile drag coefficient
C_i	curve fit constants, (i - 1,2,3)
C_ℓ	section lift coefficient
C_P	power coefficient, $P/\rho V_T^3 S$
$C_{P_{d_e}}$	equivalent drag power coefficient, $P_{d_e}/\rho V_T^3 S$
C_{P_I}	equivalent drag power integral
C_{P_i}	induced power coefficient, $P_i/\rho V_T^3 S$
C_T	thrust coefficient, $T/\rho V_T^3 S$
C/R	chord/radius ratio
C_{ROOT}/R	root chord/radius ratio
C_{TIP}/R	tip chord/radius ratio
C_μ	section momentum coefficient, $\frac{\dot{m}V_j}{qc}$
D	rotor diameter, ft
D_r	rotor drag, lbs
d	integral constant
d_p	section profile drag, lbs/ft
e	integral constant
FM	figure of merit, (Equation 5)
ℓ	section lift, lbs/ft
ℓ/d_e	equivalent section (two-dimensional) lift-drag ratio (Equation 1)
$\frac{d\dot{m}}{dr}$	section mass flux, slugs/second/feet
$\dot{m}$	mass flow left in blade, $\dot{m} = \dot{m}_T - \int_0^R \frac{d\dot{m}}{dr}\, dr$
$\dot{m}_T$	total mass flow rate, slugs/sec

LIST OF SYMBOLS (Continued)

N	number of blades
P_c	compressor power, ft-lbs/sec
P_{cor}	coriolis (pumping) power, ft-lbs/sec
P_{d_e}	equivalent drag power, ft-lbs/sec
P_i	induced power, ft-lbs/sec
P_{mom}	momentum drag power, ft-lbs/sec
P_p	profile power, ft-lbs/sec
P_N	rotor equivalent drag power, ft-lbs/sec
P_r	rotor drag power, ft-lbs/sec
P_T	total rotor power, ft-lbs/sec
R	rotor disk radius, ft
r	local radius, ft
S	disc area, ft^2
S_b	total blade area, ft^2
T/HP	inverse of power loading, lbs/horsepower
T/S	rotor disk loading, lbs/ft^2
t_1	C_{ROOT}/R
t_2	$(C_{ROOT} - C_{TIP})/R$
V	velocity, ft/sec
V_i	induced velocity, ft/sec
V_I	velocity of compressor inlet, ft/sec
V_j	jet velocity, ft/sec
V_T	tip velocity, ft/sec
V_∞	free stream velocity, ft/sec
x	dimensionless radius, r/R
α_i	induced angle of attack, degrees
η_c	compressor adiabatic efficiency

η_d	ducting efficiency
θ	blade twist angle, deg
μ	advance ratio, V/V_T
ρ	density, slug/ft^3
$\dot{\bar{\rho}}$	radial velocity vector, ft/sec
σ	rotor solidity, $\frac{S_b}{S}$
$\sigma(x)$	local solidity, $\frac{NC(x)}{\pi R}$
ϕ_i	induced inflow angle, $\tan^{-1}(V_i/xV_T)$
Ω	rotor rotational speed, rad/sec
$\bar{\omega}$	rotational velocity vector, rad/sec

SUMMARY

An approximate closed form analysis is used to determine the practical ideal hovering performance of a circulation control rotor. The rotor employs a cambered elliptical airfoil with a high section equivalent lift-drag ratio. This feature is shown to be critical for good hover performance. The calculated performance is compared with results from a more exact prediction theory and shown to yield good agreement. Finally, a comparison is made with a rotor using a standard NACA 0012 section. It is demonstrated that a circulation control rotor can achieve comparable hover efficiency to a conventional rotor but over a much greater thrust range.

INTRODUCTION

There is a present need to quantify the hover efficiency for a Circulation Control Rotor (CCR). A methodology will be established to determine the maximum obtainable figure of merit of a CCR and to make a relative comparison between a conventional helicopter rotor system utilizing a NACA 0012 airfoil and a blown elliptical airfoil section. The maximum figure of merit defined in this report is in fact a "practical ideal" figure of merit which a rotor could obtain if designed purely for hover. The significance of such an analysis is to provide a datum by which more practical rotor designs may be compared. The latter will generally vary from the ideal hover design due to the inevitable compromises for forward flight, autorotation, structure and dynamics.

In order to quantify the hover performance closed form analytical expressions were developed which may be used to gain a better understanding of the factors which determine hover efficiency, Simple integral expressions are developed herein; the only major assumptions being a linear chordwise taper ratio and ideal twist.

The analysis utilizes experimental, two dimensional airfoil data and associated equivalent lift-drag ratios. This parameter is defined in such a manner as to include all rotor power losses except for the induced and coriolis (pumping) power which may be computed separately as three dimensional contributions. The equivalent lift-drag ratio (Reference 1) is given by

$$\ell/d_e = C_\ell/C_{d_e} \tag{1}$$

where the equivalent drag coefficient is defined as:

$$C_{d_e} = C_{d_p} + C_\mu \frac{V_j}{2V_\infty} + C_\mu \frac{V_\infty}{V_j} \tag{2}$$

The first coefficient, C_{d_p}, is the net profile drag on the airfoil section (including any thrusting effect of the jet sheet). The second

term, $C_\mu \frac{V_j}{2V_\infty}$, is the gas horsepower required to develop lift at the section expressed as an equivalent drag. The last term, $C_\mu \frac{V_\infty}{V_j}$, is called the "ram drag" and is a small, somewhat pessimistic quantity normally included in the definition of equivalent lift to drag ratio in order to permit a valid comparison with other airfoils (Reference 1). This term conservatively accounts for changes of fluid momentum in a real system amounting to $\int_0^1 \frac{d\dot{m}}{dx} V_\ell \, dx$, where V_ℓ is the location section velocity. In the present analysis of a rotor blade it may be interpreted as a loss of the duct air momentum attributed to the intake and compressor losses of total pressure. An additional loss term will be added under Coriolis Power (p. 10) to account for the energy expended to increase the angular momentum of the air as it passes out the duct.

SECTION DATA USED

The CC airfoil section selected for the investigation has extremely good ℓ/d_e characteristics for a blown airfoil. Its detailed characteristics and performance are described in Reference 1 while a theoretical explanation of the section performance is given in Reference 2.

The CC section geometry used in this analysis is shown in Figure 1 together with the NACA 0012, a standard helicopter reference airfoil. The corresponding variations of ℓ/d_e with lift coefficient are shown in Figures 2 and 3. Also shown in the figures are the assumed variation of the envelope of maximum ℓ/d_e. These analytical expressions are given by:

$$\ell/d_e = C_3 C_\ell \quad \text{for } C_\ell < C_\ell \text{ at } \ell/d_{e_{max}} \tag{3}$$

$$\ell/d_e = C_1 + C_2/C_\ell \quad \text{for } C_\ell > C_\ell \text{ at } \ell/d_{e_{max}} \tag{4}$$

In general, any airfoil section may be used in the analysis which can be approximated by the above expression. The numerical values of these coefficients for the two airfoils considered here are:

Circulation Control Ellipse	NACA 0012
$C_1 = -6$	$C_1 = -12$
$C_2 = 96$	$C_2 = 43.5$
$C_3 = 90$	$C_3 = 61.3$
$C_\ell = 1.0$ at $\ell/d_{e_{max}}$	$C_\ell = 0.75$ at $\ell/d_{e_{max}}$

The NACA 0012 airfoil data are from Reference 3 for high Reynolds number and standard roughness. These data are believed to be a fairly accurate representation of an actual rotor section and were found to yield very reasonable values of figure of merit, comparable to actual test values (see: CORRELATION WITH EXPERIMENTAL DATA). The NACA 0012 does not represent an optimum conventional section but is used only as a convenient datum line. It should also be noted that the airfoil characteristics are necessarily approximate because at best they only represent the mean effect of such variables as Mach number (assumed incompressible), Reynolds number, radial flow, turbulence, and manufacturing tolerances. The ℓ/d_e number approximations chosen were selected with these considerations in mind.

Clearly the CC airfoil exhibits a much greater efficiency than the reference airfoil. To a large degree this is due to turbulent boundary layer growth on the conventional airfoil which contributes to both the friction drag and form drag and virtually halves the smooth airfoil performance. Although the chordal Reynolds number is usually well within the range for laminar flow on a rotor blade in hover, boundary layer transition normally occurs near the leading edge of conventional airfoils with the notable exception of small blade pitch angles. This transition is due to the strong adverse pressure gradients associated with operation at positive angles of attack. On the other hand, a CC airfoil operates most efficiently near zero angle of attack with very favorable pressure gradients up to lift coefficient of nominally 1.5. Therefore partial

laminar flow with a practical CC rotor construction is a very feasible proposition particularly in view of a 30-50 percent reduction in Reynolds number by use of smaller chord and tip speed.

A recent series of airfoil tests conducted since the completion of the present work have further validated the airfoil data. These tests covered a larger range of Reynolds numbers with many more test points and achieved values of ℓ/d_e as high as 120. Some of these results are also shown in Figure 2. Based on this new data the CC approximation would appear to be overly conservative even if the boundary layer flow were assumed fully turbulent (i.e., doubling the skin friction drag derates the ℓ/d_e by only ten percent).

It is also important to note that recent advances in conventional airfoils have tended toward increased use of camber to improve the airfoil efficiency, but at the expense of increase pitching moments. In the CC airfoil these features are inherent in the design and because the elastic axis is near mid chord they can be realized with relatively small moments. Reference 2 discusses some of these considerations in greater detail.

With regard to the relative assumptions of the CC and NACA 0012 airfoils it is logical to assume that the NACA representation is the more accurate simply because it has worked before in correlating rotor performance. The CC characteristics assume approximately a 25 percent reduction in peak performance opposed to almost 50 percent for the NACA 0012. However, it is not logical in any way to derate the CC by the same amount because the lift and drag mechanisms are quite different as discussed briefly above. It is, in any event, very gratifying that the agreement between experiment and theory for the NACA 0012 and between the present theory and detailed theory for the CCR are both in good agreement.

ANALYTICAL APPROACH

The objective is to define an optimum envelope of figure of merit versus thrust coefficient. This envelope does not represent any single design but rather an upper limit for all possible configurations. It

represents that maximum which could ideally be achieved by a given design at one value of thrust coefficient. To generate this envelope, the blade twist is varied so that at each thrust coefficient the blade section works at the angle of attack for best efficiency at the required section lift coefficient. The required lift coefficient is determined to give the ideal spanwise loading for minimum induced power. The minimum induced power approach will yield very close to the minimum hover power because at practical rotor thrust coefficients the induced power amounts to about two thirds of the total power required. In theory, under certain specialized conditions, it is possible to achieve a somewhat lower power consumption by working the airfoil at a lift coefficient which yields smaller profile power and slightly higher induced power. However, such gains are very marginal and certainly not within the accuracy of the present work.

In addition, the effect of rotor solidity and blade taper ratio are evaluated. Here it is assumed that the chord varies linearly from root to tip. The combinations of rotor solidity and blade taper ratio are identified which will achieve the best efficiency at a specified thrust coefficient.

General expressions are defined for each component of rotor power from which simplifying assumptions are made to perform the actual calculations. However, it will be shown in the following development that these assumptions are sufficiently accurate for the present purpose and in fact, agree surprisingly well with a more exact analysis. This latter analysis includes such effects as: (1) internal ducting losses as a function of internal duct geometry and obstructions, slot geometry, duct shape, friction coefficient, duct Mach number, centrifugal compression, temperature and heat transfer effects; (2) non-uniform induced velocity distribution computed by the Lock-Goldstein method modified to account for the concentrated tip vortex; (3) variable section characteristics as a function of thickness-chord ratio, camber, angle of attack, blowing coefficient, slot height to chord ratio, slot height to trailing edge radius ratio, and local Mach number. Obviously such a degree of refinement is necessary for a detailed design study, but at the same time, by its very nature it is quite cumbersome and would require

enormous computer time to make the present type of study. Furthermore, the closed form expressions developed herein permit a basic understanding of the hover problem, clearly showing the contribution of each term. In particular, the importance of the section equivalent lift-drag ratio in determining overall rotor efficiency is shown.

HOVER EFFICIENCY AND GOVERNING EQUATIONS

FIGURE OF MERIT

The efficiency of a rotor in hover is defined by the Figure of Merit:

$$FM = \frac{\text{Ideal Induced Power}}{\text{Total Rotor Power}} \tag{5}$$

$$= \frac{C_T^{3/2}}{\sqrt{2}C_p}$$

Efficient hovering rotors typically operate at values of FM $\simeq$ 0.7.

If the disc loading and altitude are known the power loading, T/HP (lbs/horsepower), may be determined from:

$$T/HP = \frac{550\ FM}{\sqrt{T/(2\rho S)}} \tag{6}$$

This parameter is plotted in Figure 4 as a function of disc loading and Figure of Merit for the standard and "hot day" conditions.

GENERAL POWER EQUATIONS

The general equation for the total rotor power required in flight is:

$$P_T = P_p + P_c + P_i + P_{cor} + P_{mom} + P_r \tag{7}$$

where each of the power components are given below:

Profile: $$P_p = N \int_0^R V(r)\, dp(r) \cos \phi_i(r)\, dr \tag{8}$$

Compressor; including duct efficiency:

$$P_c = \frac{N}{2} \int_0^R \frac{d\dot{m}}{dr}(r) \frac{V_j(r)}{\eta_c \eta_d} dr \tag{9}$$

Induced:

$$P_i = N \int_0^R V(r) \ell(r) \sin \phi_i(r) \, dr \tag{10}$$

Coriolis:

$$P_{cor} = 2N\Omega^2 \int_0^R r \, \dot{m}(r) \, dr \tag{11}$$

Inlet Momentum: $$P_{mom} = \dot{m}_T V_I \tag{12}$$

Rotor Drag: $$P_r = D_r V_\infty \tag{13}$$

In hover the last two terms, Equations (12) and (13) are zero. It is assumed that the rotor will be shaft driven so that the torque is, in general, positive. Each of the remaining equations (8 through 11) will be developed into a closed form in the next section.

Induced

The calculation of induced power is greatly simplified in the present analysis by the assumption that the rotor can generate constant downwash velocity and hence develop minimum induced power. In practice this may be very nearly accomplished by adjusting the spanwise distribution of slot height (Reference 4). From annulus momentum theory the induced power is given by:

$$P_i = N \int V_i \, d\ell = 4\pi\rho \int_0^R V_i^3 \, r dr \tag{14}$$

and for constant V_i an ideal power coefficient can be derived as:

$$C_{p_i} = 0.707 \, C_T^{3/2} \tag{15}$$

The corresponding ideal distribution of lift is quite difficult to calculate[1] and the complex vortex theory must be employed. This has, in fact, been done with the aim of deriving a higher order expression for the lift distribution which could be used in the analysis. Unfortunately the final expression led to extremely involved power integrals which defeated the purpose of the study, therefore a simpler first order approach was necessitated. These results are given below without derivation in the interest of brevity:

Higher Order Distribution:

$$C_{\ell}(x) = \frac{\frac{4C_T}{\sigma(x)}}{\sqrt{.25 + C_T/2}\cdot\cos(\tan^{-1}(2\sqrt{C_T/2}))}\sqrt{\frac{x - x^2}{x^2 + C_T/2}} \qquad (16)$$

First Order Distributions[2]:

$$C_{\ell}(x) = \frac{4C_T}{\sigma(x)x}\ , \text{ for } 0.3 \leq x \leq 1.0 \qquad (17)$$

$$C_{\ell}(x) = \frac{4xC_T}{.3\sigma(x)}, \text{ for } 0 \leq x < 0.3 \qquad (18)$$

Figure 5 compares the spanwise lift distributions given by the exact vortex theory, the higher order expression and the first order expression, respectively. It may be noted that significant variations occur only in the tip region. The present analysis therefore uses the first order distribution to calculate power which yields slightly optimistic induced power but slightly conservative profile power so that the two effects are essentially cancelling. It is emphasized that the first order distribution is only a convenience for calculation and that the correct distribution for an actual minimum induced power design is given by equation 16. Present conventional rotors have come close to the minimum power assumption in

---

[1] simple momentum considerations incorrectly yield lift coefficient distributions proportion to 1/x leading to finite tip loading and incorrect twist loading. This error is most prominant at high thrust coefficient.

[2] The choice of the 0.3 station as the point of maximum lift was determined from considerations of the maximum circulation grading on a wing of finite span.

this analysis and would come much closer still if they employed the non linear twist implied by equation 16.

Profile and Compressor

The concept of equivalent lift-drag ratio will be used in this formulation to avoid the difficulties involved with separate profile and compressor power calculations. These difficulties are primarily due to the effect of slot height changes. It has been shown by experiment (Reference 7) that a change of slot height for the same momentum flux, or C_μ, produces significant changes in lift, drag and compressor power but very little variation of the parameter ℓ/d_e defined by Equation (1). An added benefit of this method is to provide a direct means of relating section efficiency to rotor hover efficiency (Figure of Merit) for <u>any airfoil</u>.

The equivalent drag power is defined as:

$$P_p + P_c = P_{d_e} = \frac{\rho N R^2 V_T^3}{2} \int_0^1 \frac{C/R\ C_\ell x^3}{\ell/d_e}\, dx \qquad (19)$$

in coefficient form,

$$C_{P_{d_e}} = \frac{N}{2\pi} \int_0^1 \frac{C/R\ C_\ell x^3}{\ell/d_e}\, dx \qquad (20)$$

Now from the previous assumptions of uniform inflow, the variation of C_ℓ with C_T and x may be written as:

$$\frac{C}{R} C_\ell = \frac{4\pi C_T}{Nx}, \quad 0.3 \le x \le 1.0 \qquad (21)$$

$$\frac{C}{R} C_\ell = x\ \frac{4\pi C_T}{.3N}, \quad 0 \le x < .3 \qquad (22)$$

Furthermore, assuming a linear variation of blade chord as:

$$\frac{C}{R} = t_1 - t_2 x \tag{23}$$

where $t_1 = C_{ROOT}/R$, $t_2 = (C_{ROOT} - C_{TIP})/R$ and recalling the definition of ℓ/d_e from Equations 3 and 4 the profile and compressor power can be expressed as a function of x and C_ℓ only. Due to the discontinuity in the definition of ℓ/d_e the evaluation of the integral must be accomplished in parts as shown schematically in Figure 6. Thus, the total profile and compressor power can be expressed as:

$$C_{p_{d_e}} = C_{p_{I_1}} + C_{p_{I_2}} + C_{p_{I_3}} + C_{p_{I_4}} \tag{24}$$

The evaluation of each of these integrals is carried out in Appendix A.

Coriolis

The last term of the approximate analysis is the pumping or coriolis power (which is required to increase the angular momentum of the air as it flows out the blade duct toward the tip) is:

$$P_{cor} = \Omega N \int_0^R r dF_{cor} \tag{25}$$

where the coriolis force is obtained from the equations of motion for a differential element of mass, dm;

$$d\bar{F}_{cor} = (2\bar{\omega} \times \dot{\bar{\rho}})\, dm$$

$$\text{or} \quad \left| dF_{cor} \right| = 2\Omega V dm$$

Where $V = \dot{\bar{\rho}}$ is the duct velocity.

A change of variables in made by noting:

$$Vdm = V(r)\ \rho(r)\ A(r)\ dr = \dot{m}\ (r)\ dr,$$

where $\dot{m}(r)$ is the mass flux in the blade so that the mass flow rate of the air in the duct at any radial station r (taking s as an integration variable) is:

$$Vdm = \left[\dot{m}_T - \int_0^r \left(\frac{d\dot{m}}{ds}\right) ds\right] dr$$

Therefore:

$$P_{cor} = 2\Omega^2 N \int rVdm = 2\Omega^2 N \int_0^R r\left[\dot{m}_T - \int_0^r \left(\frac{d\dot{m}}{ds}\right) ds\right] dr \qquad (26)$$

where $\dot{m}_T$ is the total mass flow rate out of a blade

$$\dot{m}_T = \int_0^R \frac{d\dot{m}}{dr}\, dr$$

and $\frac{d\dot{m}}{dr}$ is the mass flux per foot of span.

The momentum coefficient is next defined generally by:

$$C_\mu(r) = \frac{\frac{d\dot{m}}{dr} V_j(r)}{q(r)c(r)} \qquad (27)$$

and for hover by,

$$C_\mu(x) = \frac{\frac{1}{R}\frac{d\dot{m}}{dx} V_j}{\frac{\rho}{2} x^2 V_T^2 c(x)}$$

A small approximation is next made in order to solve the power integral in closed form by simply assuming V_j = const. It should be noted that the assumption of constant V_j implies that the total head losses due to friction are identically balanced by the head rise due to centrifugal compression. The power expended to achieve this centrifugal compression is called coriolis or pumping power.[3]

A detailed internal flow analysis of a constant chord blade (Reference 4) indicates that the above assumption is approximately correct for a ratio of $V_j/V_T \simeq 1.2$. In actuality the total pressure (hence jet velocity) first drops at the inboard section and then rises outboard to a higher value than initially. Consequently the effect of assuming an average value of V_j over the entire blade is somewhat pessimistic but certainly within the accuracy of the present analysis.

The mass efflux out the slot is:

$$\frac{d\dot{m}}{dx} = \frac{\rho V_T^2 R}{2V_j} \left[c(x)\, x^2\, C_\mu(x) \right]$$

And the integral in Equation (26) is then as follows:

$$\dot{m}_T = \int_0^R \frac{d\dot{m}}{dr}\, dr = \int_0^1 \frac{d\dot{m}}{dx}\, dx$$

$$\dot{m}_T = \frac{\rho V_T^2 R}{2V_j} \int_0^1 c(x) x^2 C_\mu(x) dx \qquad (28)$$

---

[3]Under ideal isentropic conditions the power expended for pumping is regained by a reduced compressor power requirement (which is due in turn to the centrifugal compression). The present analysis assumes that friction losses prevent any increase in duct pressure and hence preclude any compressor power reduction.

By next employing the original assumption that the airfoil is operating at the (constant) angle of attack for maximum ℓ/d_e along the blade, then the lift coefficient can be approximated as:

$$C_\ell = c_4 C_\mu + c_5 \tag{29}$$

where: c_4 is the lift curve slope with blowing coefficient and c_5 is the lift contribution due to either camber of angle of attack.

All of the necessary terms of (26) are now available:

$$\dot{m}_T = \frac{\rho V_T^2 R^2}{2V_j c_4}\left[\int_0^1 C_\ell \frac{c(x)}{R} x^2 dx - c_5 \int_0^1 \frac{c(x)}{R} x^2 dx\right] \tag{30}$$

and from (26)

$$\int_0^r \left(\frac{d\dot{m}}{ds}\right) ds = \frac{\rho V_T^2 R^2}{2V_j c_4}\left[\int_0^x s^2 \left(\frac{c(s) C_\ell}{R}\right) ds - c_5 \int_0^x s^2 \frac{c(s)}{R} ds\right] \tag{31}$$

The evaluation of the above integrals are carried out in Appendix A with the coriolis power coefficient obtained as:

$$C_{p_{COR}} = \frac{P}{\rho \pi R^2 V_T^3} = \frac{4 C_T V_T}{c_4 V_j}\left(\frac{.0109 t_1 - .00262 t_2}{t_1 - .3 t_2} + 0.12399\right) \tag{32}$$

$$- \frac{N V_T c_5}{\pi V_j c_4}\left(0.1 t_1 - .0833 t_2\right)$$

For the special case of constant chord, zero angle of attack and zero camber the above expression simplifies to:

$$C_{p_{COR}} = \frac{.54 C_T V_T}{c_4 V_j} \tag{33}$$

Hence the pumping power can be reduced by increasing the ratio $c_4 = \Delta C_\ell / \Delta C_\mu$, and by increasing the ratio of V_j/V_T (higher duct pressure, lower RPM). It increases linearly with increasing thrust coefficient.

RESULTS

The results will be discussed in terms of the dimensionless rotor quantities of figure of merit and thrust coefficient for various values of rotor taper ratio and solidity. The thrust coefficient-solidity ratio, C_T/σ, will be used to discuss the general effect of blade loading (although this parameter does not fully represent the effect of varying solidity). These dimensionless quantities may easily be converted into dimensional terms of power loading and average blade loading by using Figures 4, 7 and 8.

CORRELATION WITH EXPERIMENTAL DATA

The validity of the present method can be partially determined by comparison with actual test data for two NACA 0012 rotors with taper ratios of 2 to 1 and 3 to 1 (References 5 and 6). The pertinent characteristics of these rotors are listed below.

	NACA 0012	NACA 0012
Taper ratio	2:1	3:1
Root chord/radius	0.253	0.267
Tip chord/radius	0.127	0.103
Twist, deg	-12.0	-8.0
σ	0.099	0.095
Number of blades	2	2

The rotors were tested at various tip Mach numbers. As the present comparison is based on the low speed section characteristics a correlation was attempted with the lowest tip speed case of $M_{TIP} = 0.45$. Only

one point of comparison is provided by each test corresponding to the thrust coefficient for which the blade twist is given by the momentum theory expression[4]:

$$\theta(x) = \alpha_i(x) - \alpha_i(1.0)$$

where α_i is the local induced angle, $\alpha_i(x) = \tan^{-1}(\sqrt{C_T/2}/x)$

Using the above information the following correlations were obtained:

Taper ratio	2:1	3:1
Thrust coefficient (for ideal thrust)	.00378	.00244
Experimental Figure Merit	0.61	0.46
Calculated Figure Merit	0.60	0.46

The agreement is extremely good so that it is felt that considerable confidence may be placed in the NACA 0012 calculation as a reference point from which to compare CCR performance.

COMPARISON WITH DETAILED ANALYSIS

The detailed numerical analysis discussed previously was also used to determine the validity of the present approach. This method correlates well for standard airfoils and can therefore be used with confidence for the circulation control rotors. Detailed CC section data were input and then the rotor twist and slot distribution varied at each value of C_T in order to achieve the vortex theory ideal loading. The collective pitch and duct pressure were then varied in order to define the optimum figure of merit at each C_T. The locus of these points described the limiting envelope of figure of merit for the constant chord case chosen.

The results are shown in Figure 9 where it may be seen that, in general, the agreement is satisfactory over the thrust coefficient range of practical interest (approximately .005 - .015). For reference a similar optimization has been done which includes compressibility effects

[4] Again it is noted that the momentum theory does not yield the correct twist distribution for minimum induced power. It was apparently used for the check case design considered above.

(obtained from Reference 7) and is shown in the figure also. No attempt has been made to calculate the compressibility effect using the present analysis although it would only require adjustment of the ℓ/d_e coefficients.

EFFECT OF SOLIDITY AND TAPER RATIO

All results given are for a four bladed rotor. The locus of optimum figure of merit for values of root Chord/Radius = .03, .05, .07, and .09 are shown in Figure 10. Several interesting trends may be noted:

(i) The maximum figure of merit alwys occurs for the constant chord case and rather high C_T/σ.

(ii) At lower C_T/σ (which may be the practical operating values) the effect of taper is beneficial signifying important related improvements in blade weight and high speed performance.

(iii) The thrust coefficient range for good efficiency is quite large and is maintained even at low blade aspect ratio[5]. This is a significant result for highly loaded propellers such as lift fans, ducted propellers or compressors.

DESIGN EXAMPLE AND COMPARISON WITH CONVENTIONAL ROTOR

As a typical design example consider a helicopter rotor with the following features:

Disc Loading, 10 pounds/feet^2
Blade Loading, 150 pounds/feet^2
Tip Speed, 600 feet/second

The corresponding dimensionless values (from Figures 7 and 8) are:

$$C_T = .0117$$
$$C_T/\sigma = .165$$
$$\sigma = .067$$

[5] The analysis probably becomes increasingly inaccurate as aspect ratio decreases and thrust coefficient increases so that the quantitative results under extreme conditions are probably optimistic

Using Figure 10c it may be noted that a blade with $C_{ROOT}/R = .07$ and $C_{TIP}/R = .035$ will provide a maximum figure of merit of 0.86 for the CCR. From Figure 4 this is seen to correspond to a power loading of about 10.2 pounds/horsepower (S.L.S.), quite good for a helicopter rotor system. Moreover, it should be noted that due to the greater section thickness, taper ratio (2 to 1) and more ideal load distribution the rotor would be expected to have a lower rotor weight fraction than a conventional system[6].

A conventional rotor design would typically operate at a lower value of C_T/σ (due to blade stall). Referring the Figure 11 for the NACA 0012 it may be noted that two design possibilities arise: (1) For maximum efficiency (FM = 0.81) a solidity of $\sigma = .0827$ is chosen. In this case only a small power penalty is paid compared with the CCR. However, the increase in solidity would probably result in a considerable rotor weight penalty[7]; (2) If solidity is reduced the weight penalty also reduces but at the expense of power. At $\sigma = .0756$, the figure of merit has rapidly dropped to FM = 0.73. A comparison of the two rotors for the constant chord case (approximately equal blade weight) is shown for reference in Figure 12.

Finally it should be recalled that these results are strictly for an optimum hover design. The cruise mode necessitates large reductions in twist and variation in thickness ratio in order to achieve a reasonable hover-cruise performance compromise. In general, for a conventional rotor this implies operation considerably off the optimum described, herein. In contrast the CCR can still achieve close to the ideal hover loading with zero twist (by use of slot height variation) so that a significantly smaller hover performance decrement would be anticipated, (Reference 8).

---

[6] A 30-percent thickness ratio ellipse has 10 times the flapwise stiffness and 7 times the torsional stiffness of a NACA 0012 section of equal weight.

[7] Rotor blade weight historically varies with the blade area to the 1.36 power while the total rotor group weight historically varies in proportion to $N^{1.27}(\text{Blade Wt.})^{0.95}$.

CONCLUSIONS

An integral solution for the envelope of maximum efficiency of a Circulation Control Rotor in hover has been developed and shows good agreement with a more exact numerical solution. The concept of equivalent section lift-drag ratio was shown to be a valid parameter for comparing blown and unblown airfoils.

The Circulation Control Rotor has very good hovering efficiency over a large range of rotor thrust. The maximum values are somewhat higher than the conventional NACA 0012 and occur over a much wider thrust range.

Linear blade taper is beneficial (compared to untapered) in the useful rotor thrust coefficient range.

A Circulation Control Rotor with relatively thick airfoil sections, linear taper and optimum spanwise loading appears to offer substantial improvements in rotor hover performance.

Aviation and Surface Effects Department
Naval Ship Research and Development Center
Bethesda, Maryland 20034
August 1971

APPENDIX A

EVALUATION OF INTEGRALS

Determination of a closed form solution for the profile and compressor power is a lengthy process which includes the evaluation of four integrals. Equation A1 is the basic integral to be evaluated with the limits of integration described schematically in Figure 6.

$$C_{p_{d_e}} = \frac{N}{2\pi} \int_0^1 \left[\frac{C/R \; C_\ell x^3}{\ell/d_e} \right] dx \tag{A1}$$

where:

$$\frac{C}{R} C_\ell = \frac{4\pi C_T}{Nx} \text{ , for } 0.3 \leq x \leq 1.0 \tag{A2}$$

$$\frac{C}{R} C_\ell = x\left(\frac{4\pi C_T}{.3N}\right), \text{ for } 0 \leq x < 0.3 \tag{A3}$$

$$\frac{C}{R} = t_1 - t_2 x \tag{A4}$$

$$t_1 = C_{ROOT}/R \tag{A5}$$

$$t_2 = (C_{ROOT} - C_{TIP})/R \tag{A6}$$

$$\ell/d_e = c_3 C_\ell \text{ for } C_\ell < C_\ell \text{ at } \ell/d_{e_{max}} \tag{A7}$$

$$\ell/d_e = c_1 + c_2/C_\ell \text{ for } C_\ell > C_\ell \text{ at } \ell/d_{e_{max}} \tag{A8}$$

By substitution of Equations A2 through A8 in Equation A1, the power integral can be expressed totally as a function of C_ℓ and x.

For case I:

$$C_\ell < C_\ell \text{ at } \ell/d_{e_{max}} \; ; \; 0 \leq x \leq x_{o_1}$$

$$C_{p_{I_1}} = \frac{N}{2\pi c_3} \int_0^{x_{o_1}} (-t_2 x^4 + t_1 x^3)\, dx \qquad \text{(A9)}$$

$$= \frac{N}{2\pi c_3} \left[-\frac{t_2}{5} x^5 + \frac{t_1}{4} x^4 \right]_0^{x_{o_1}} \qquad \text{(A10)}$$

For case II:

$$C_\ell > C_\ell \text{ at } \ell/d_{e_{max}} \; ; \; x_{o_1} < x \leq 0.3$$

$$C_{p_{I_2}} = \frac{N}{2\pi} J^2 \int_{x_{o_1}}^{0.3} \frac{x^5}{d + ex} dx \qquad \text{(A11)}$$

where:

$$J = \frac{4\pi C_T}{.3N}$$

$$d = c_2 t_1$$

$$e = c_1 \left(\frac{4\pi C_T}{.3N} \right) - c_2 t_2$$

$$w = d + ex$$

$$C_{p_{I_2}} = \frac{NJ^2}{2\pi e^6} \left[5d^4 w - 5w^2 d^3 + \frac{10}{3} w^2 d^2 - \frac{5}{4} w^4 d^4 + \frac{w^5}{5} - d^5 \ln(w) \right]_{x_{o_1}}^{0.3} \qquad \text{(A12)}$$

For case III:

$$C_{\ell} > C_{\ell} \text{ at } \ell/d_{e_{max}} \; ; \; 0.3 < x \leq x_{o_2}$$

$$C_{p_{I_3}} = \pi C_T \int_{0.3}^{x_{o_2}} \frac{x^2}{a + bx + cx^2} \, dx \tag{A13}$$

where:

$$a = c_1$$

$$b = \frac{c_2 t_1 N}{4\pi C_T}$$

$$c = \frac{-c_2 t_2 N}{4\pi C_T}$$

$$q = 4ac - b^2 \quad q < 0$$

$$X = a + bx + cx^2$$

$$C_{p_{I_3}} = \pi C_T \left[\left(\frac{x}{c} - \frac{b}{2c^2} \log X + \left(\frac{b^2 - 2ac}{2c^2} \right) \cdot \frac{-2}{\sqrt{-q}} \tanh^{-1} \left(\frac{2cx + b}{\sqrt{-q}} \right) \right) \right]_{0.3}^{x_{o_2}} \tag{A14}$$

for $t_2 = 0$, constant chord blade

$$C_{p_{I_3}} = \frac{\pi C_T}{b^3} \left[.5(a + bx)^2 - 2a(a + bx) + a^2 \log (a + bx) \right]_{0.3}^{x_{o_2}} \tag{A15}$$

For case IV:

$$C_\ell < C_\ell \text{ at } \ell/d_{e_{max}} \; ; \; x_{o_2} < x \leq 1.0$$

$$C_{p_{I_4}} = \frac{N}{2\pi c_3} \int_{x_{o_2}}^{1.0} (-t_2 x^4 + t_1 x^3)dx \qquad \text{(A16)}$$

$$C_{p_{I_4}} = \frac{N}{2\pi c_3} \left[-\frac{t_2}{5} x^5 + \frac{t_1}{4} x^4 \right]_{x_{o_2}}^{1.0} \qquad \text{(A17)}$$

The pumping or coriolis power is determined in a similar manner by evaluating each of the integrals separately.

The basic equation to be evaluated is:

$$\int_o^x \frac{d\dot{m}}{ds} \Big) ds = \frac{\rho V_T^2 R^2}{2V_j c_4} \left[\int_o^x \frac{s^2 c(s) C_\ell}{R} \, ds - c_5 \int_o^x \frac{s^2 c(s)}{R} \right] ds \qquad \text{(A18)}$$

where C_ℓ is defined by Equations (A2) through (A6). Now the first integral on the R.H.S. yields:

$$\frac{\rho V_T R^2}{2V_j c_4} \left[\int_o^x \frac{s^2 c(s) C_\ell}{R} \right] ds = \frac{\rho V_T^2 R^2}{2V_j c_4} (I_1 + I_2) \qquad \text{(A19)}$$

where

$$I_1 = \frac{4\pi C_T}{N(.3)^2 C/R(.3)} \left(\frac{t_1 x^4}{4} - \frac{t_2 x^5}{5} \right) \text{ for } 0 \leq x < 0.3$$

and

$$I_2 = \frac{4\pi C_T}{N} \left(\frac{x^2}{2} - \frac{(.3)^2}{2} \right) \text{ for } 0 \leq x \leq 1.0$$

The second integral is evaluated as follows:

$$-c_5 \int_0^x \frac{s^2 c(s)}{R}\, ds = -\frac{c_5 \rho V_T^2 R^2}{2 V_j c_4} \left(\frac{t_1 x^3}{3} - \frac{t_2 x^4}{4} \right) \qquad \text{(A20)}$$

Upon substitution of Equation (A19) and (A20) into (A18) and integrating:

$$C_{p_{cor}} = \frac{P}{\rho \pi R^2 V_T^3} = \frac{4 C_T V_T}{c_4 V_j} \left(\frac{.0109 t_1 - .00262 t_2}{t_1 - .3 t_2} + 0.12399 \right) \qquad \text{(A21)}$$

$$- \frac{N V_T c_5}{\pi V_j c_4} \left(0.1 t_1 - 0.0833 t_2 \right)$$

REFERENCES

1. Williams, Robert M. and Harvey J. Howe. Two Dimensional Subsonic Wind Tunnel Tests on a 20 Percent Thick, 5 Percent Cambered Circulation Control Airfoil. Wash., Aug 1970. 23p. (Naval Ship Research and Development Center. Tech Note AL-176) (AD 877 764)

2. Williams, Robert M. Design Considerations of Circulation Control Airfoils. (Naval Ship Research and Development Center. Tech Note AL-185) (To be published)

3. Abbott, Ira H. and Albert E. von Doenhoff. Theory of Wing Sections. N.Y., Dover Publications, Inc., 1959. 693p.

4. Williams, Robert M. Some Research on Rotor Circulation Control. IN CAL/AVLABS Symposium: Aerodynamics of Rotary Wing and V/STOL Aircraft. 3rd, Buffalo, N.Y., Jun 1969. Proceedings, Vol. 2.

5. Jewel, Joseph W., Jr. and Robert D. Harrington. Effect of Compressibility on the Hovering Performance of Two 10-Foot Diameter Helicopter Rotors Tested in the Langley Full-Scale Tunnel. Wash., Apr 1958. 43p. (National Advisory Committee for Aeronautics. RM L58B19)

6. Jewel, Joseph W., Jr. Compressibility Effects on the Hovering Performance of a Two-Blade 10-Foot-Diameter Helicopter Rotor Operating At Tip Mach Numbers Up to 0.98. Wash., Apr 1960. 28p. (National Aeronautics and Space Adm. Tech Note D-245)

7. Englar, Robert J. Two-Dimensional Transonic Wind Tunnel Tests of Three 15-Percent Thick Circulation Control Airfoils. Wash., Dec 1970. 63p. (Naval Ship Research and Development Center. Tech Note AL-182) (AD 882 075)

8. Williams, Robert M. Analysis of the Hover Performance of a High Speed Circulation Control Rotor. (Naval Ship Research and Development Center. Tech Note AL-221) (To be published)

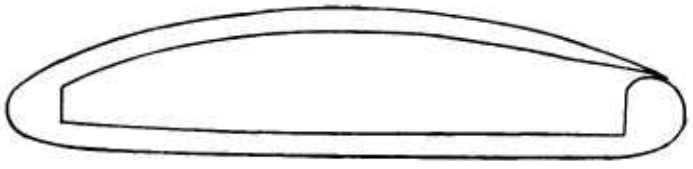

Cambered Twenty Percent Thickness Circulation
Control Ellipse

NACA 0012 Standard Reference Airfoil

Note: Chord Length for same Figure of Merit

Figure 1 - Airfoil Sections used in Analysis

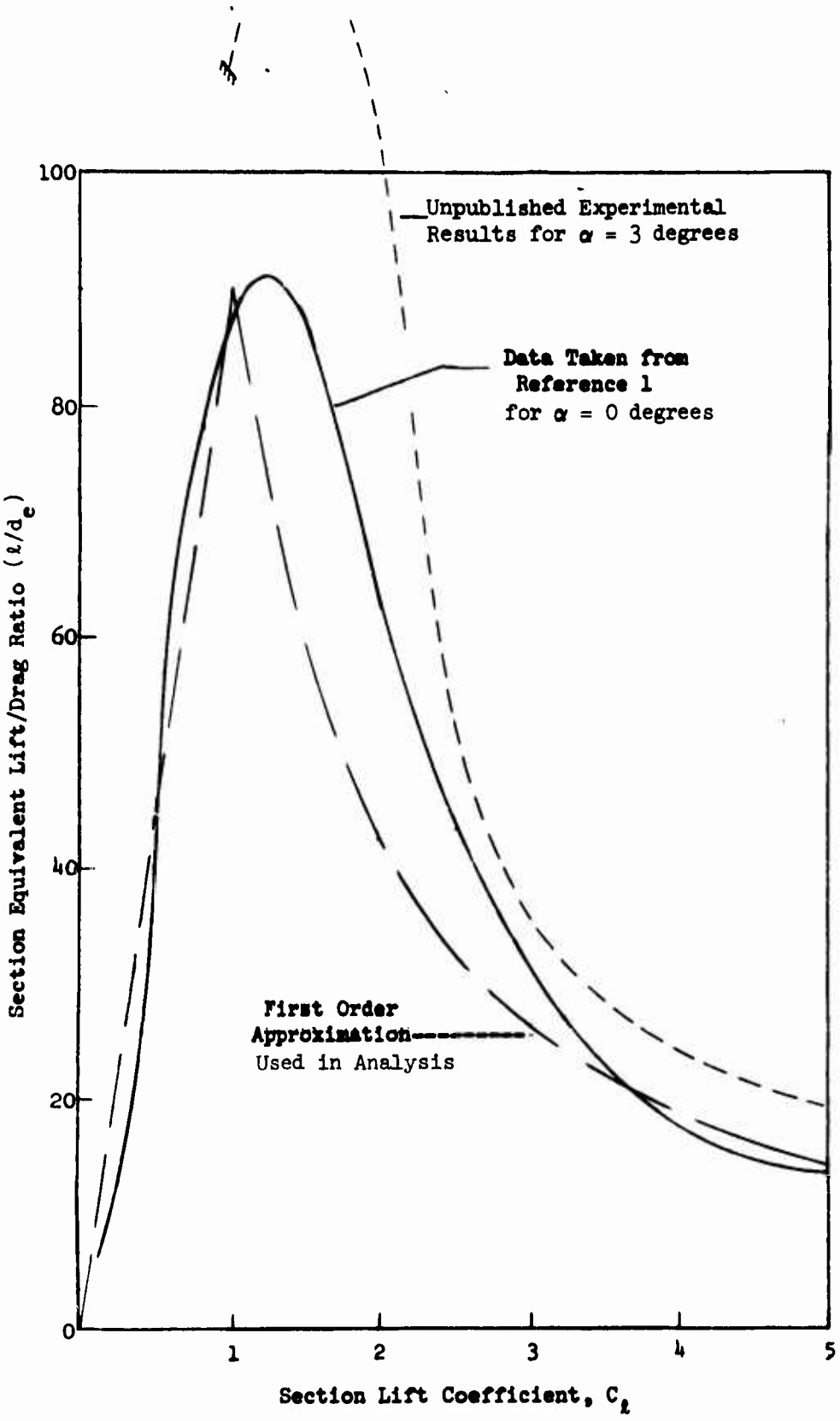

Figure 2 - Variation of Equivalent Lift-Drag Ratio for the Circulation Control Airfoil

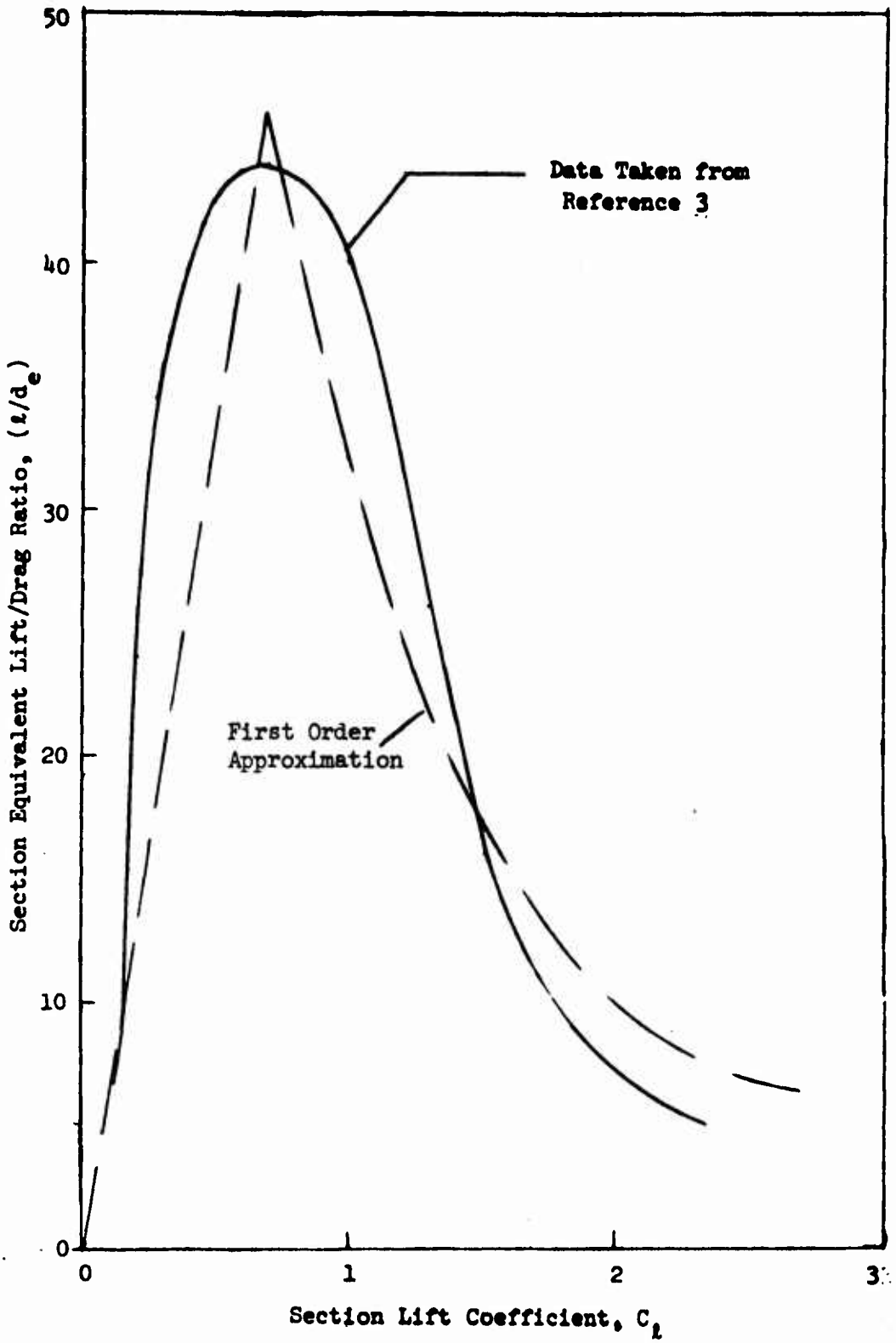

Figure 3 - Variation of Equivalent Lift-Drag Ratio for the NACA 0012 Airfoil

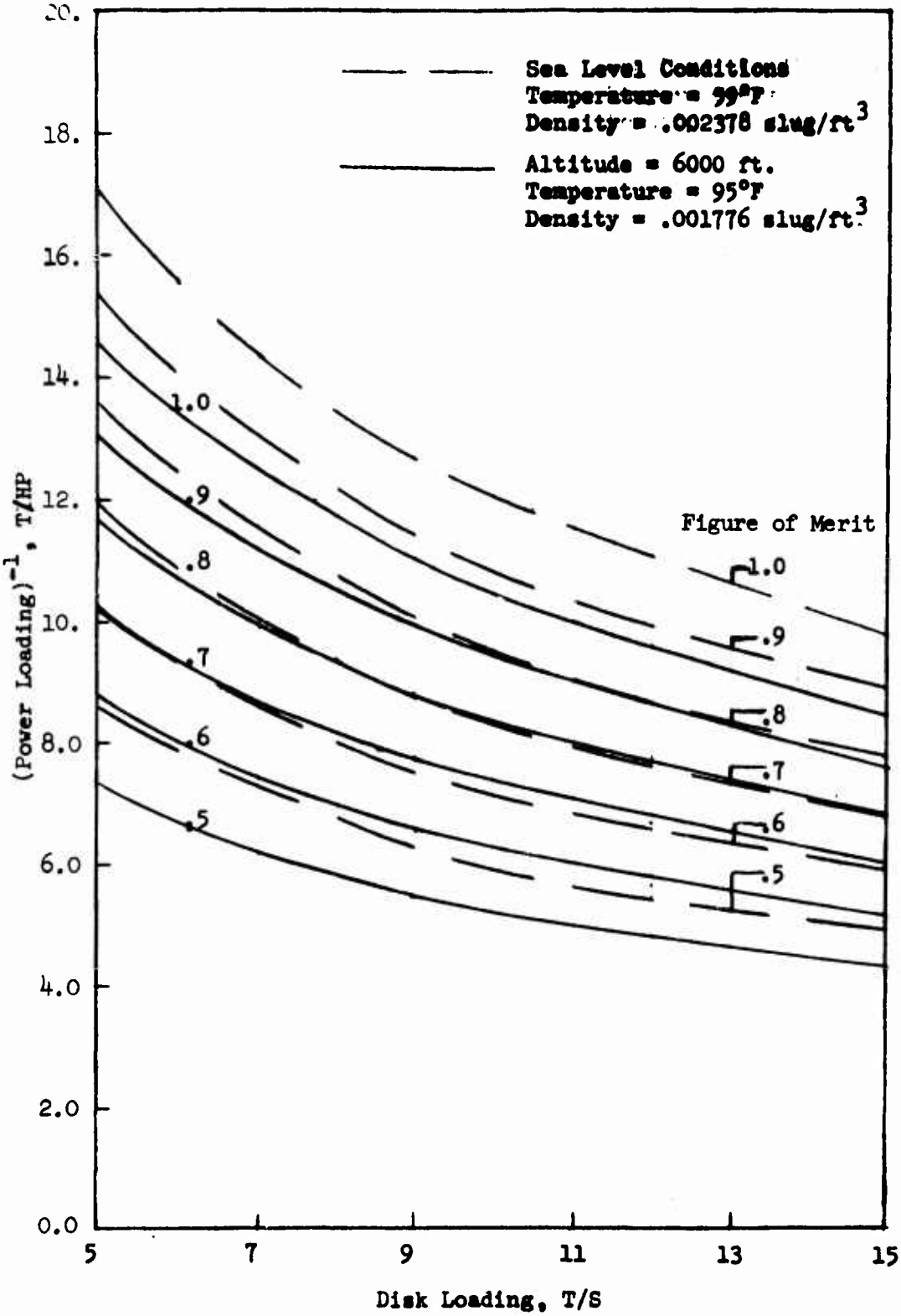

Figure 4 - Variation of Hover Power Loading with Disc Loading for Various Figures of Merit

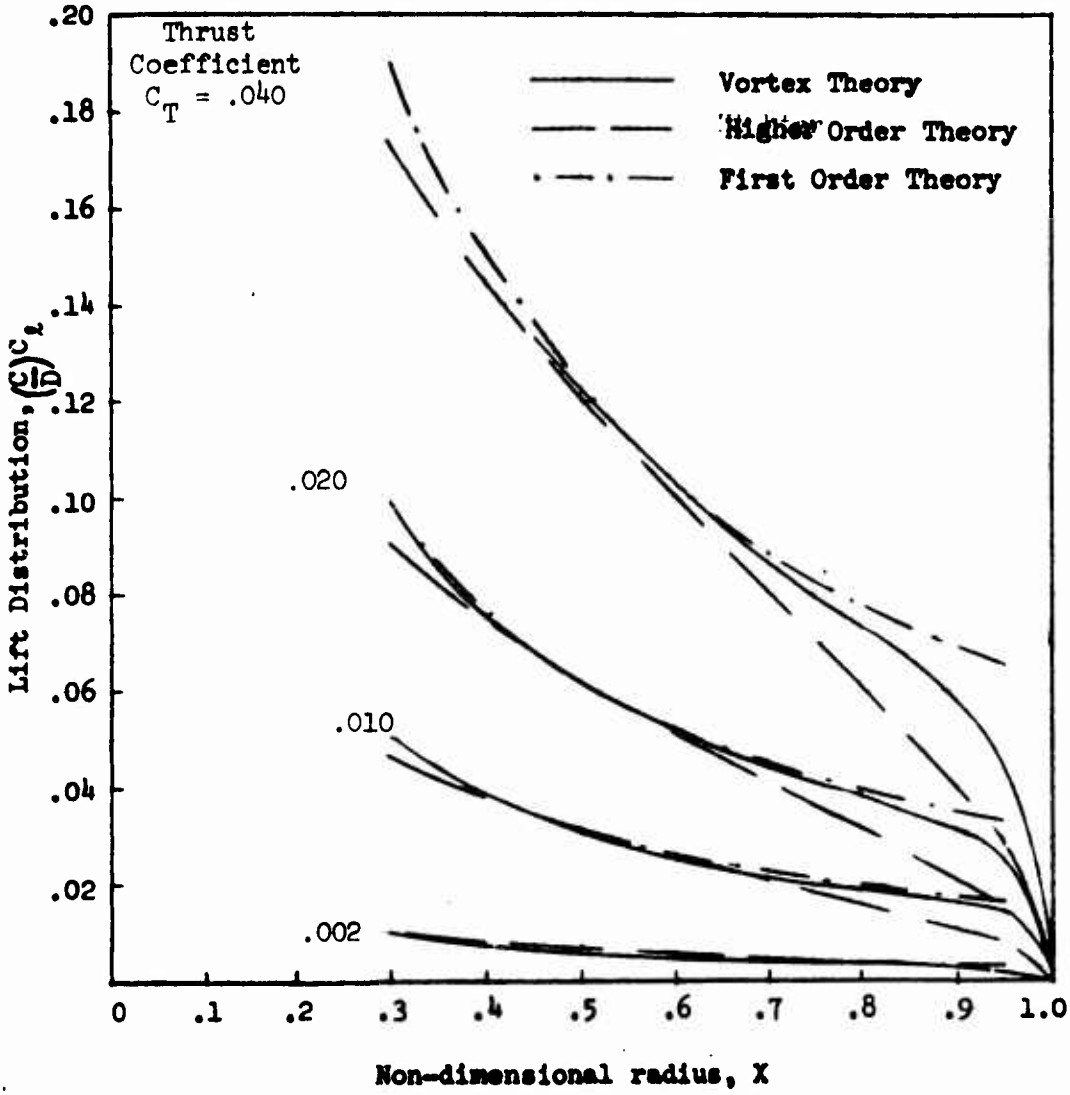

Figure 5 - Variation of Lift Distribution with Radius for Various Theories (4 Blades)

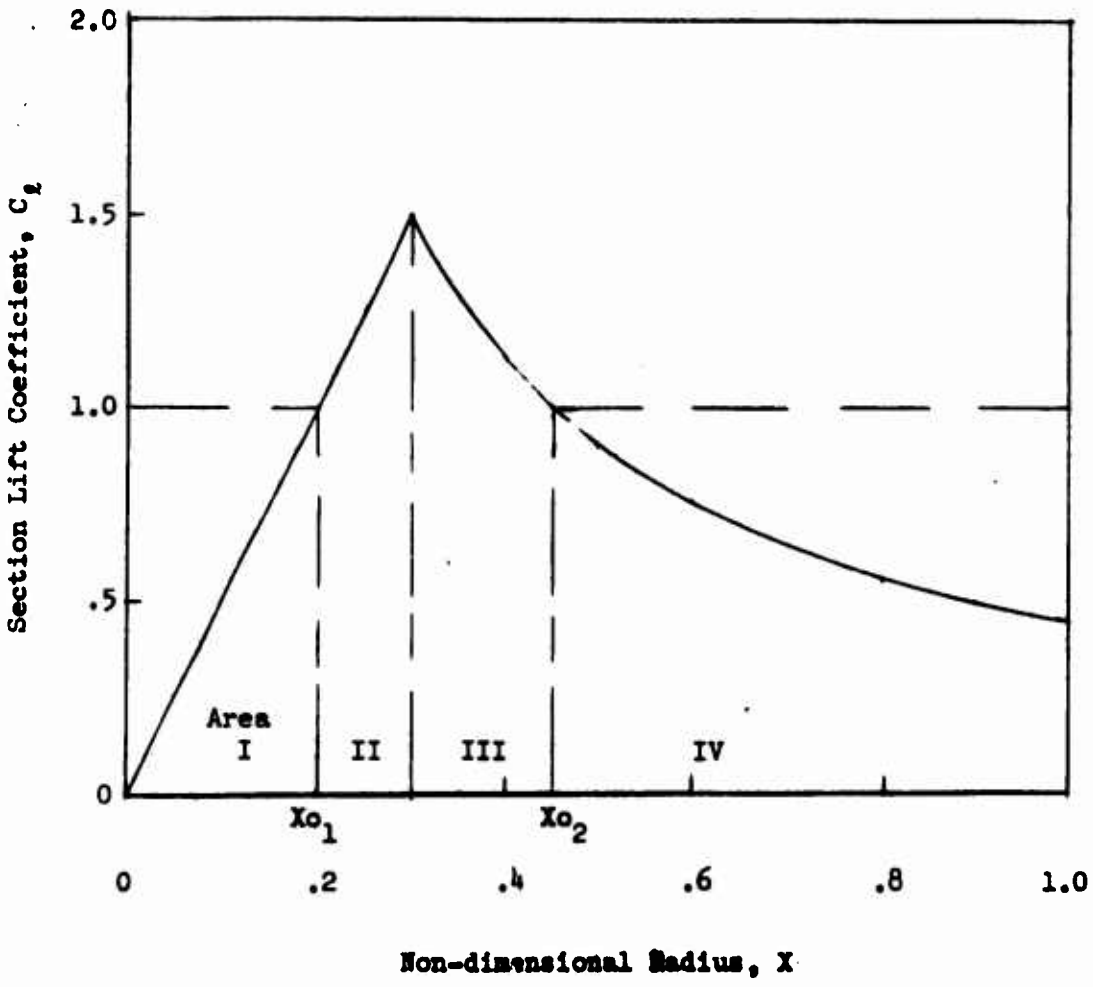

Figure 6 - Typical Variation of Section Lift Coefficient with Radius and the Associated Integrals

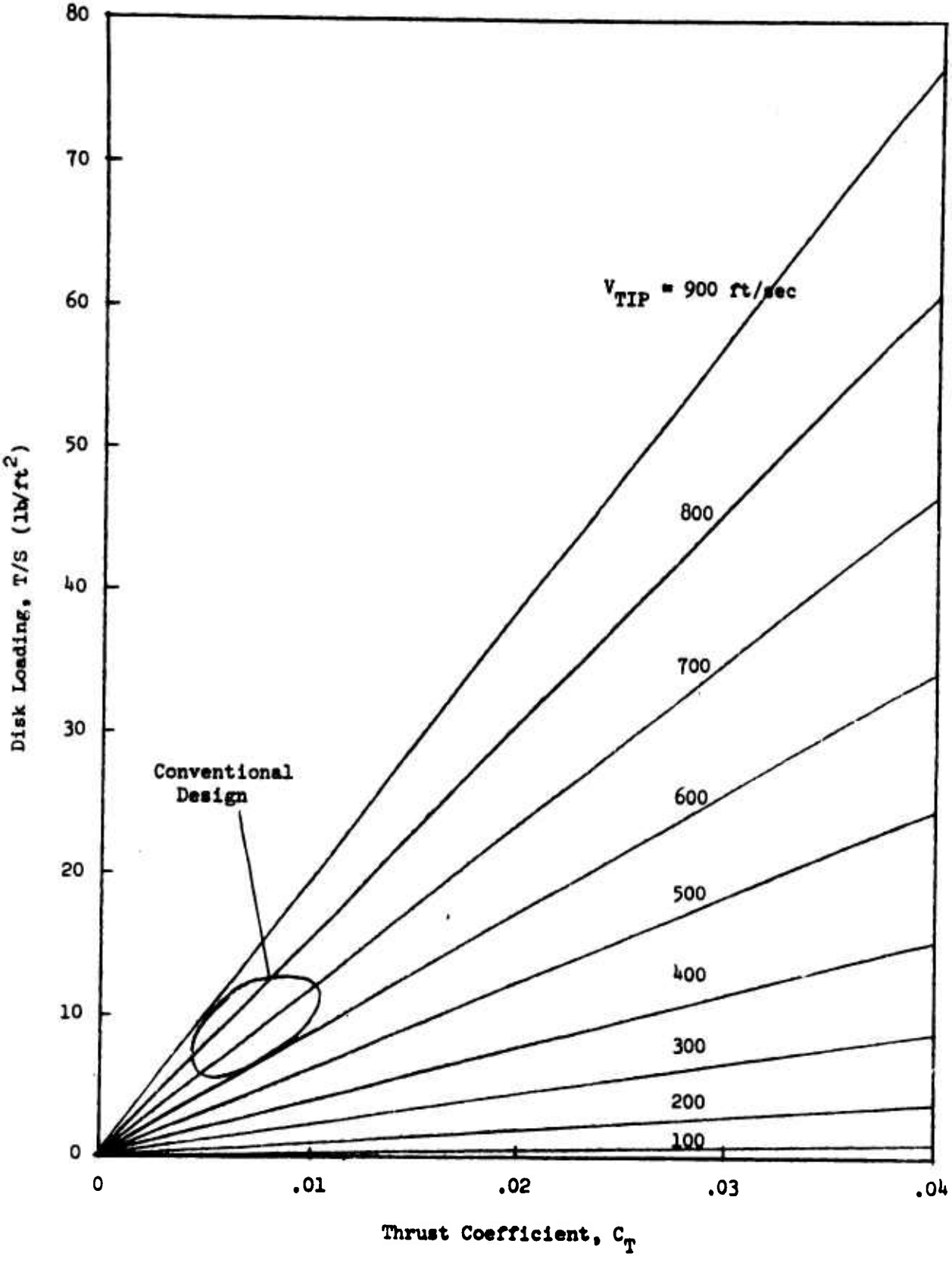

Figure 7 - Conversion Plot for Disc Loading

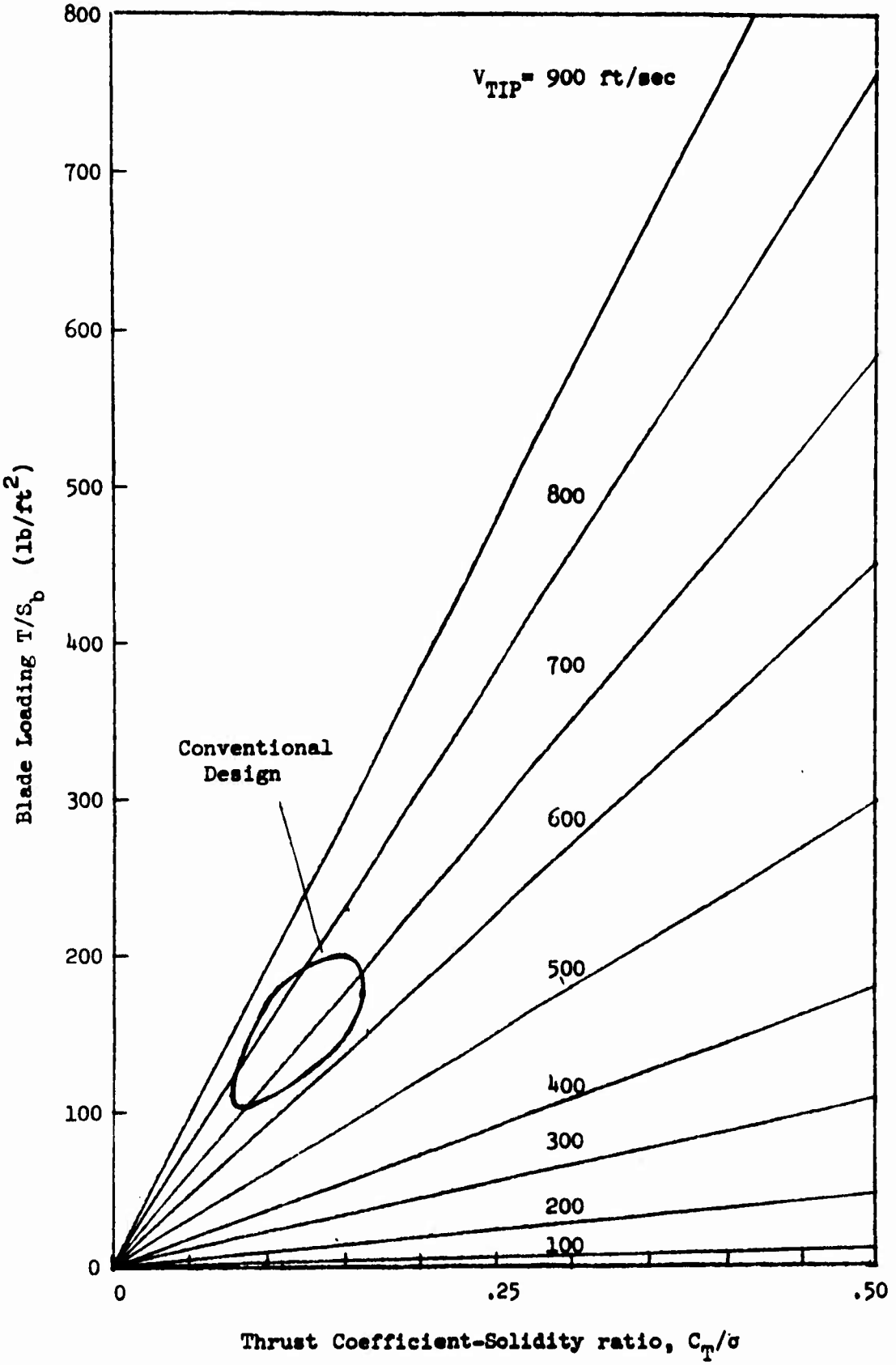

Figure 8 - Conversion Plot for Average Blade Loading

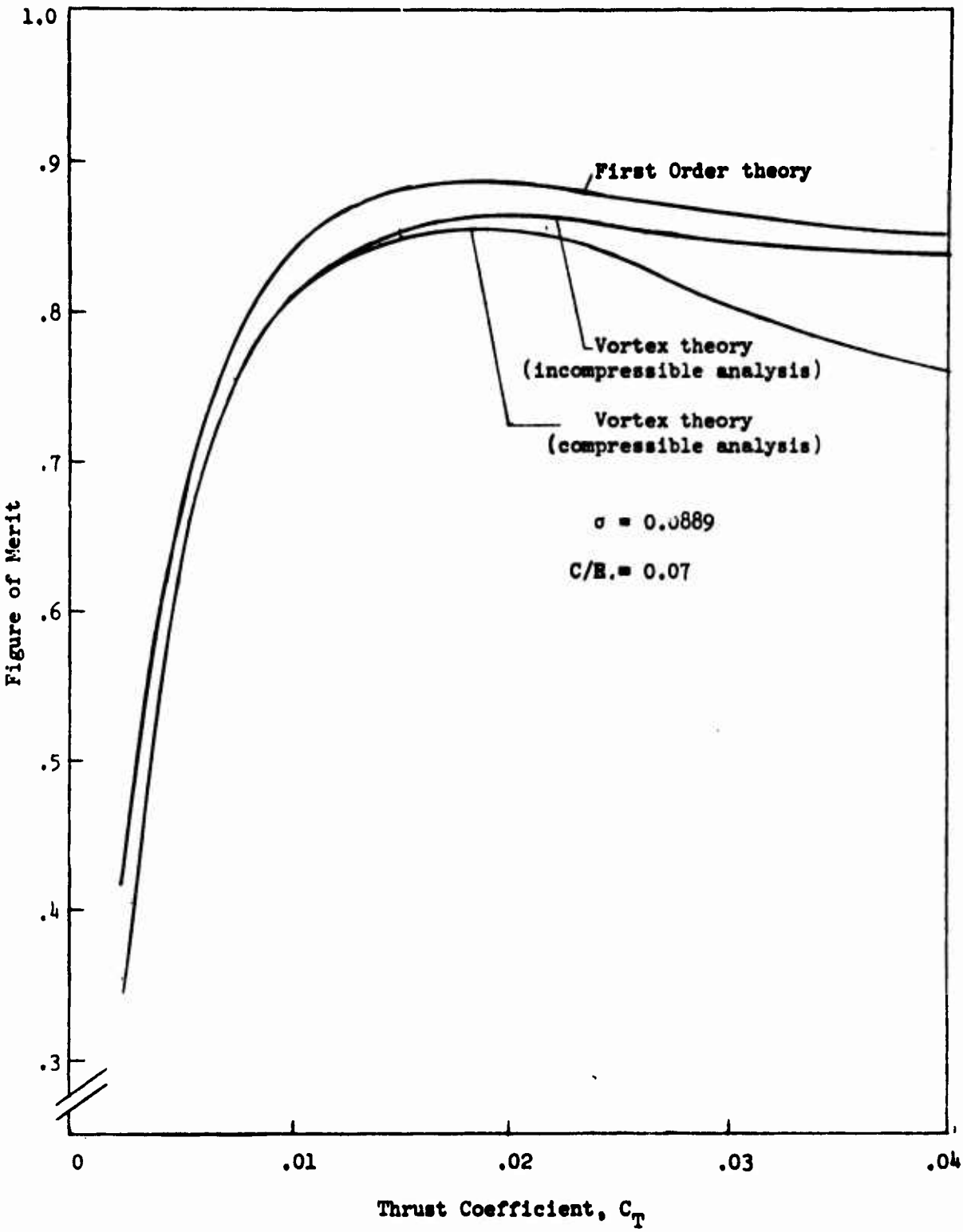

Figure 9 - Variation of Figure of Merit with Thrust Coefficient for Various Theories

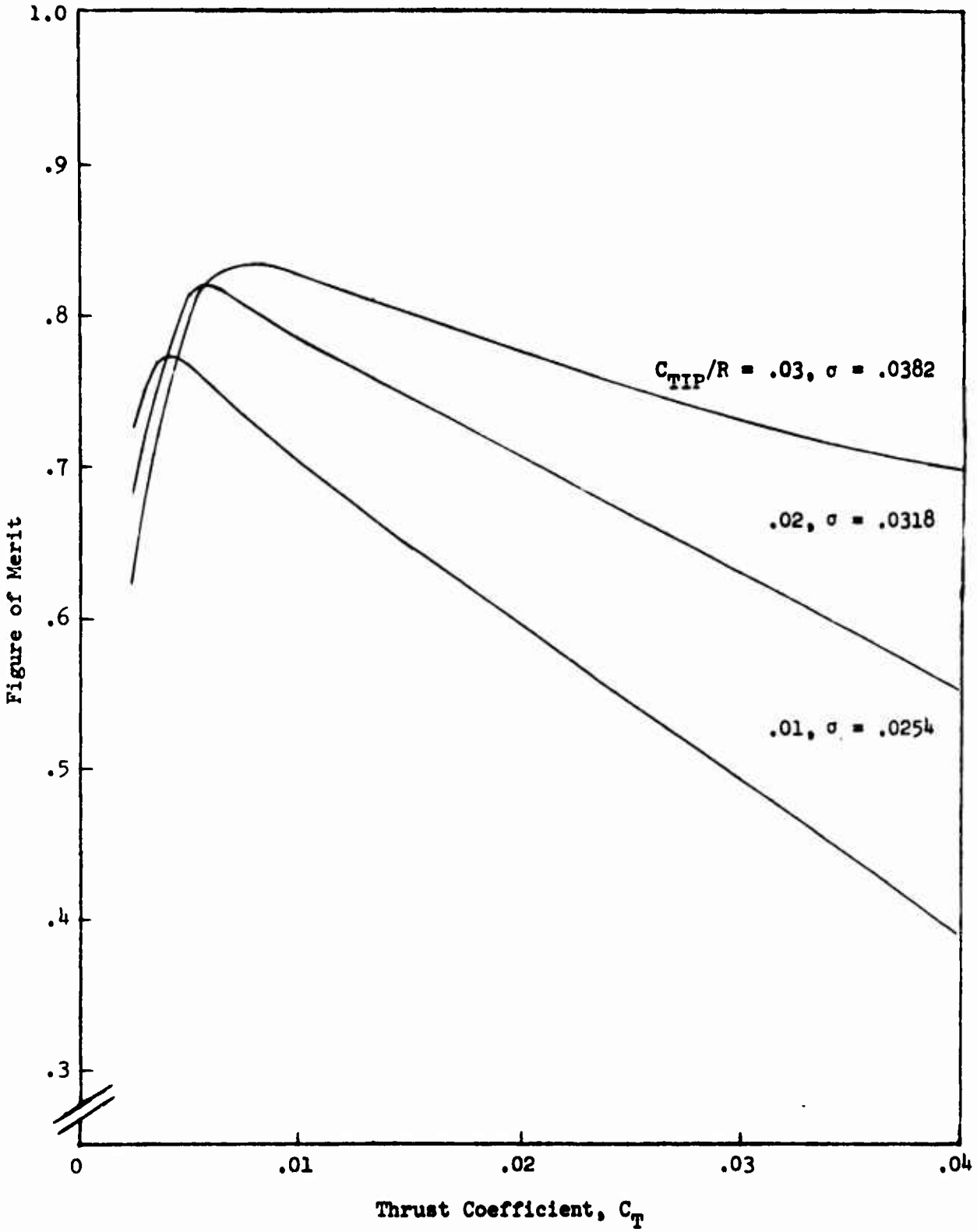

Figure 10 - Locus of Optimum Figure of Merit for Circulation Control ROTOR (a) C_{ROOT}/R = .03

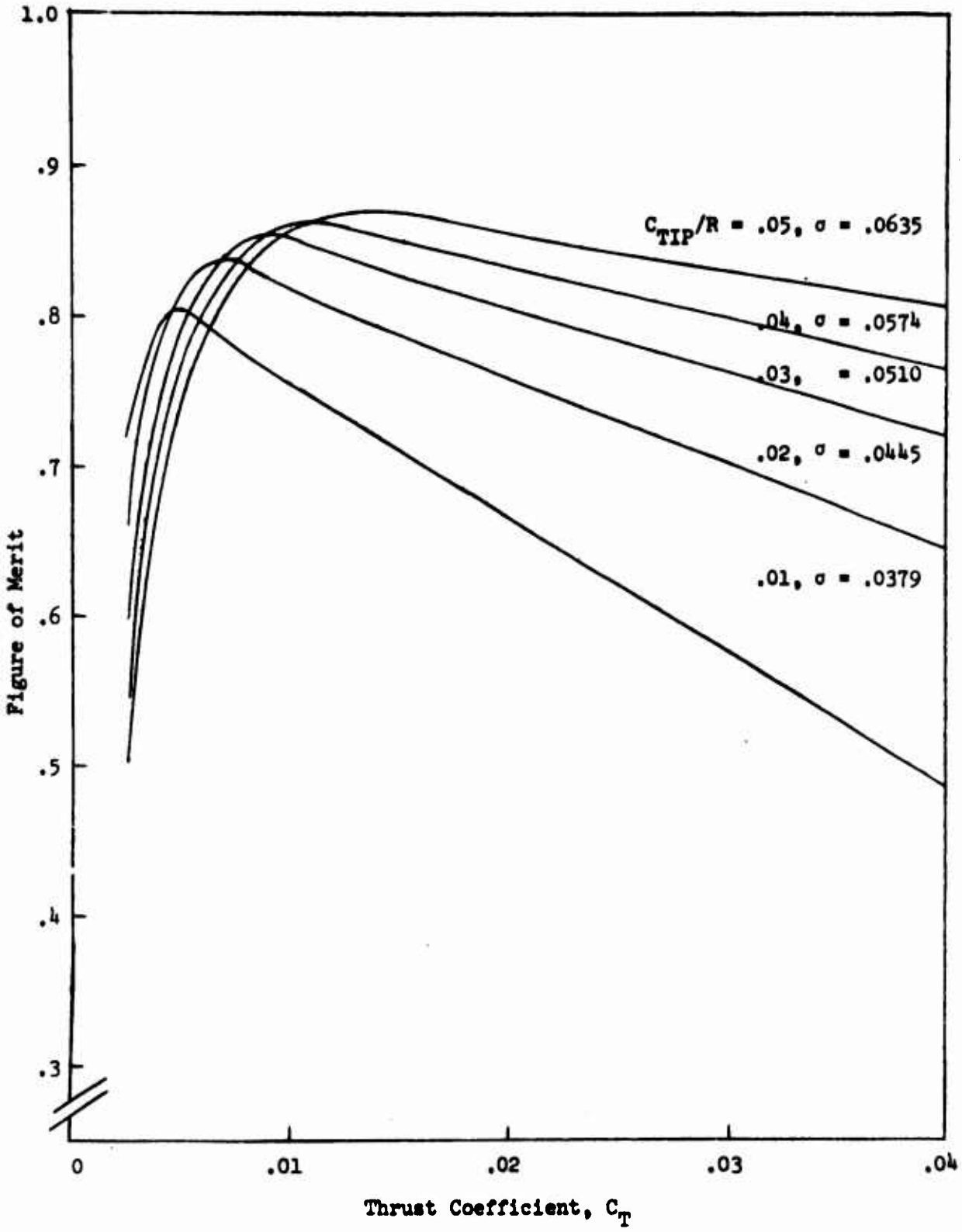

Figure 10 (Continued)
(b) C_{ROOT}/R = .05

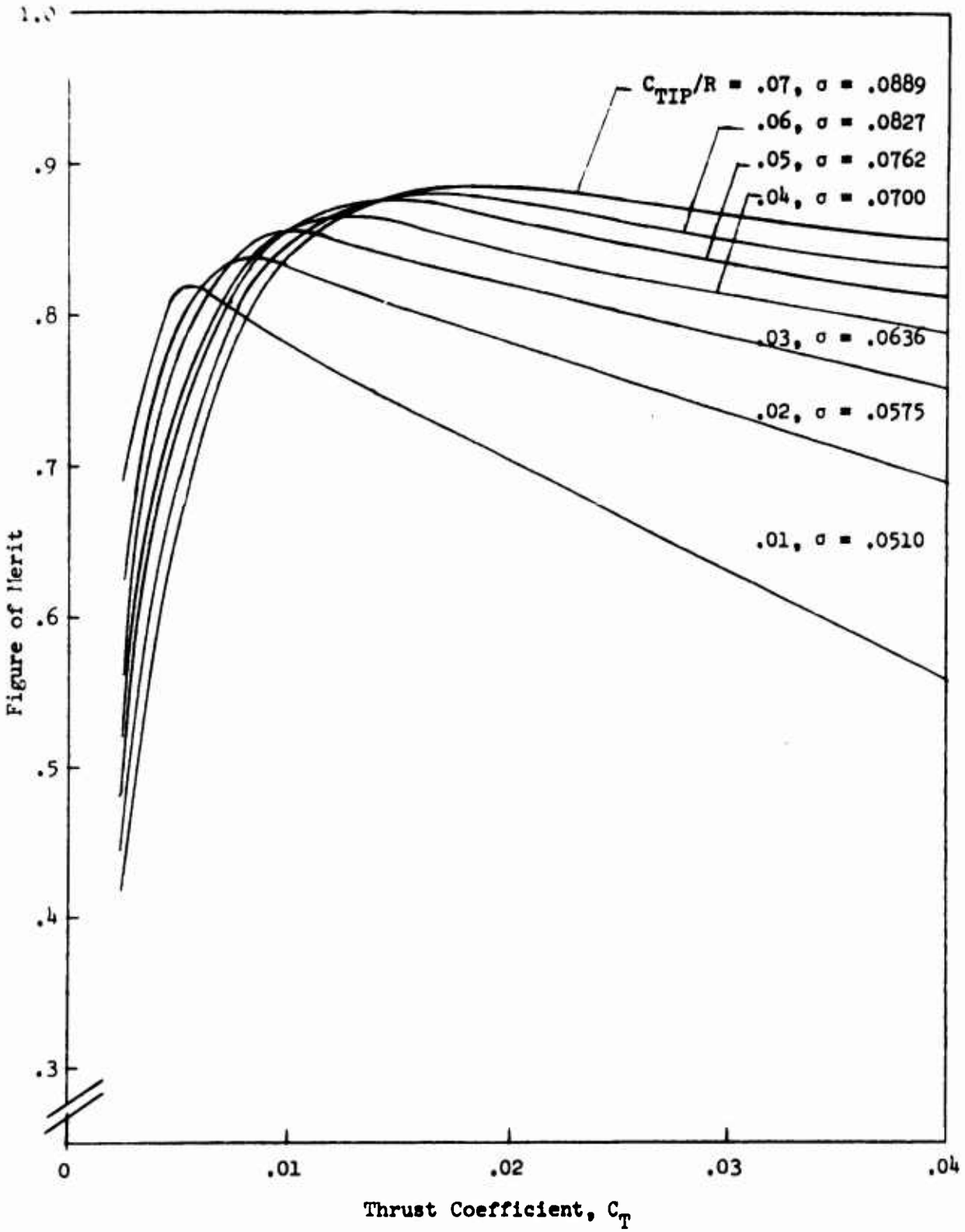

Figure 10 (Continued)

(c) C_{ROOT}/R = .07

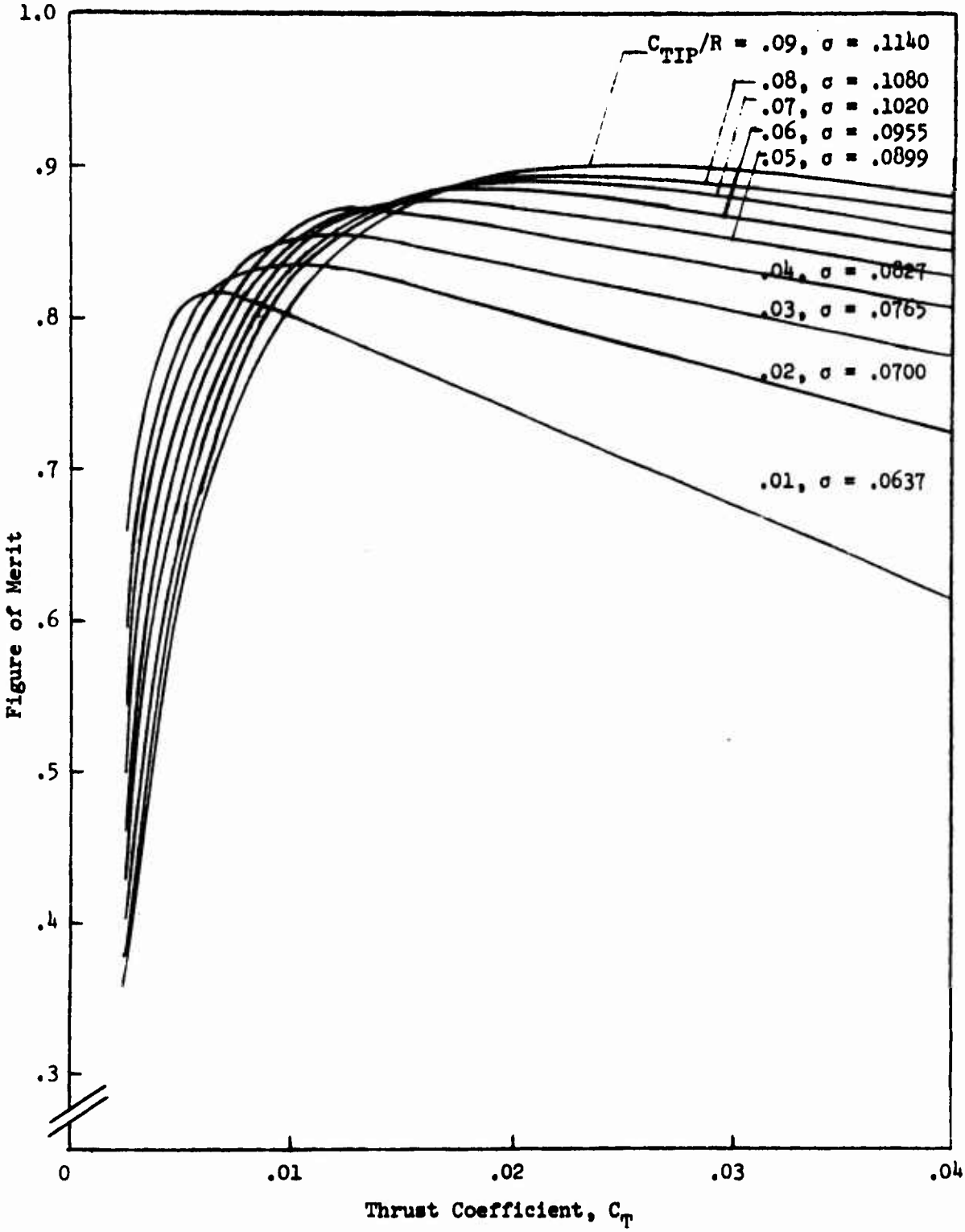

Figure 10 (Concluded)

(d) C_{ROOT}/R = .09

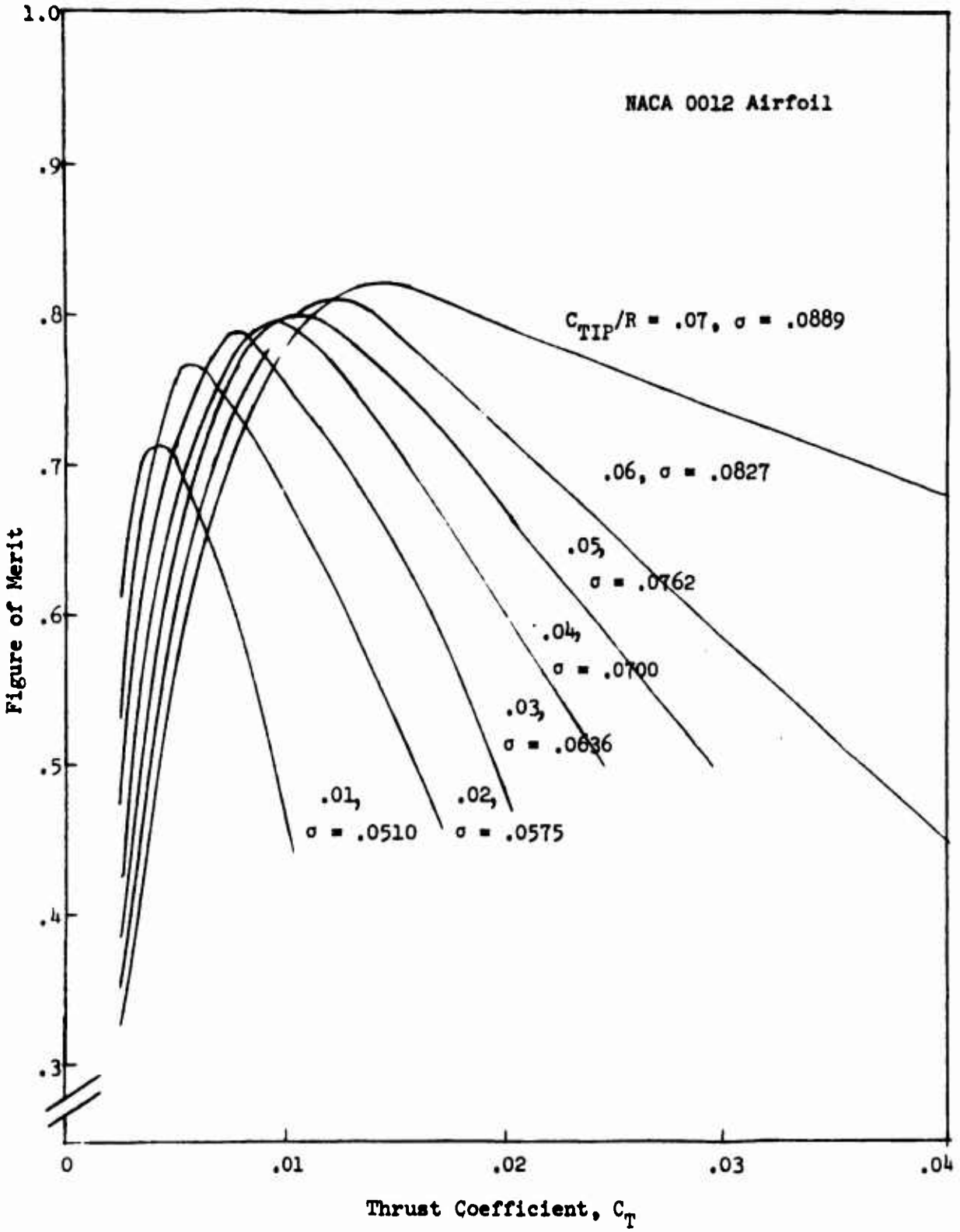

Figure 11 - Locus of Optimum Figure of Merit for NACA 0012 Rotors,

C_{ROOT}/R = .07

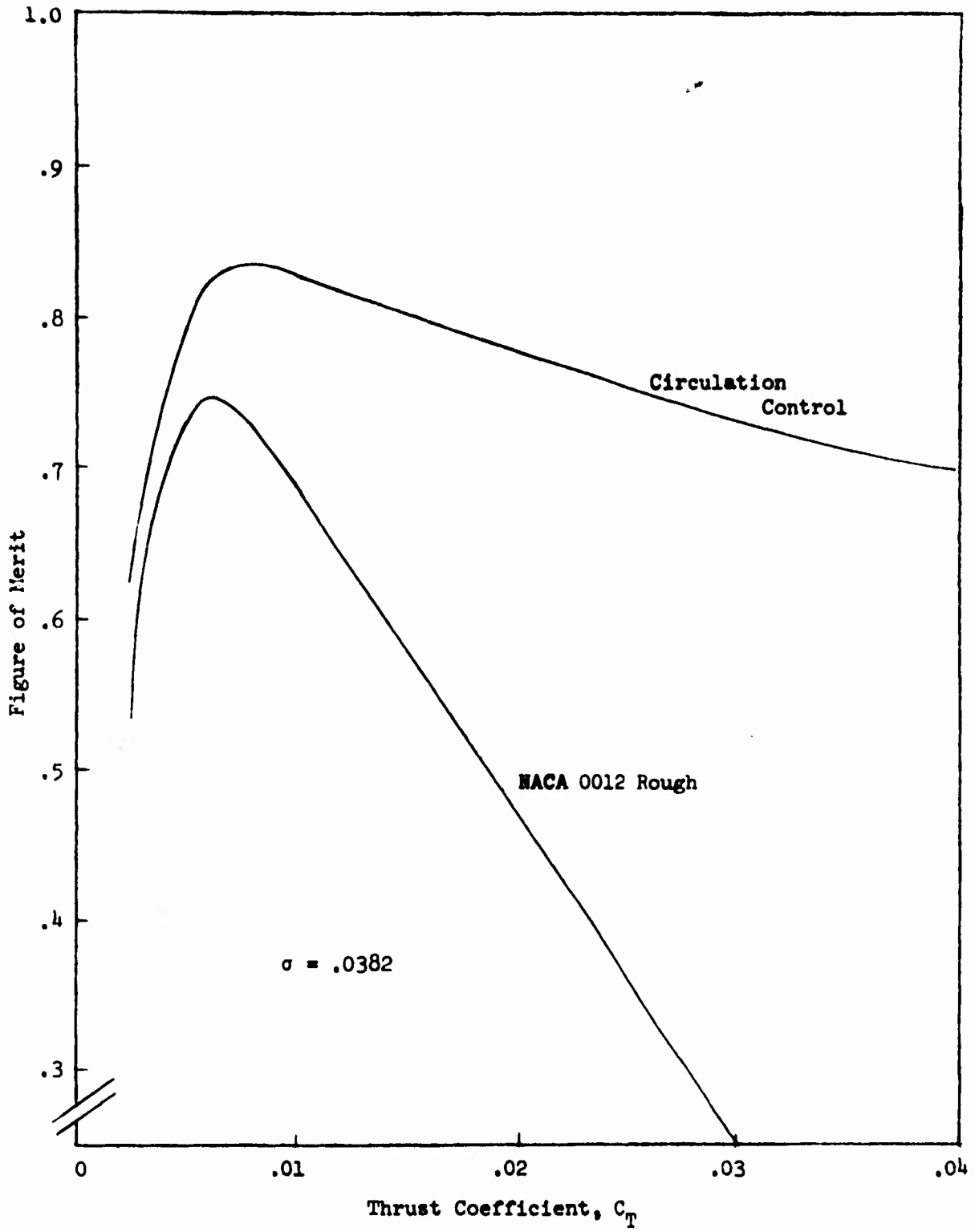

Figure 12 - Variation of Figure of Merit with Thrust Coefficient for NACA 0012 and Circulation Control Rotor

(a) C/R = .03

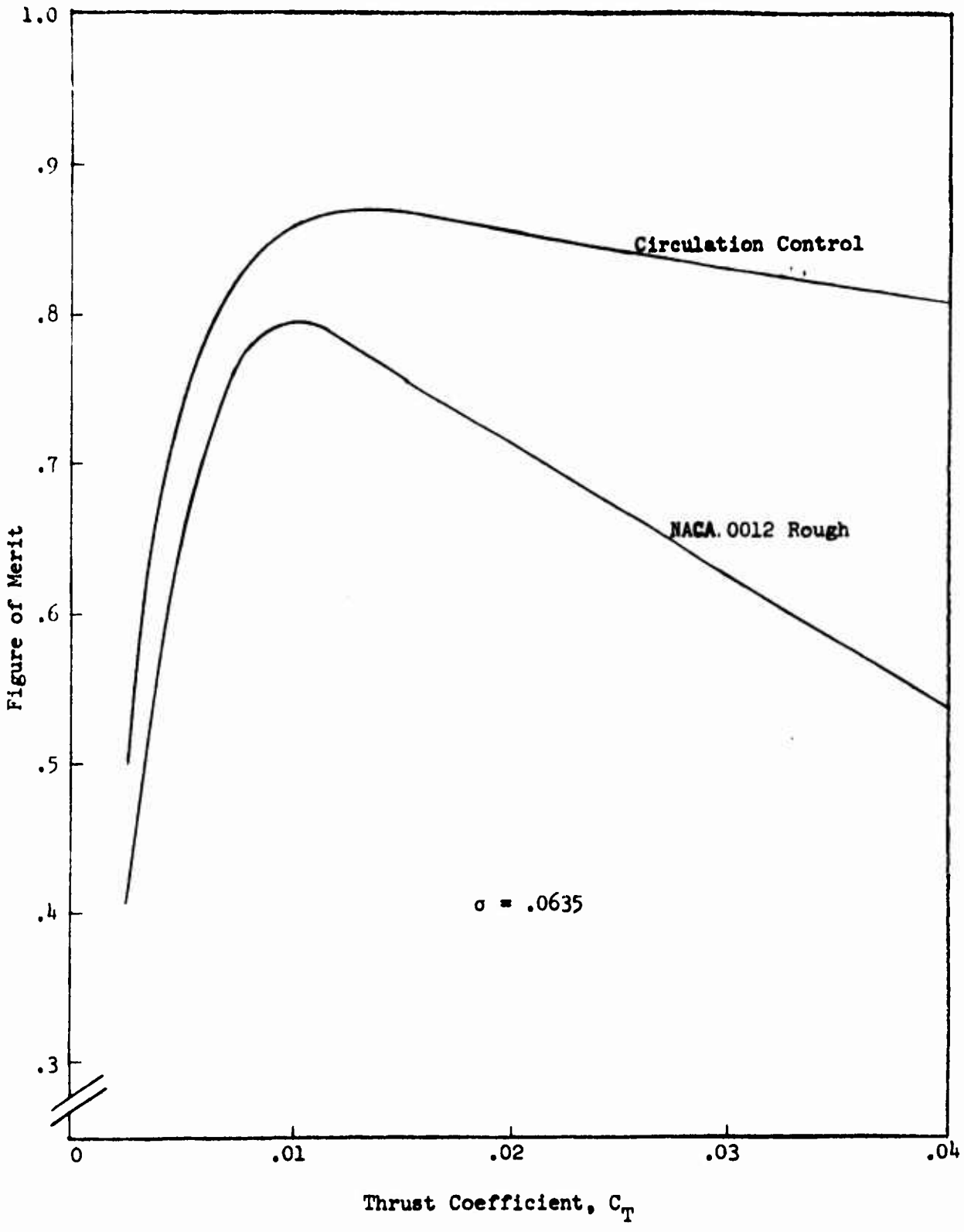

Figure 12 (Continued)
(b) C/R = .05

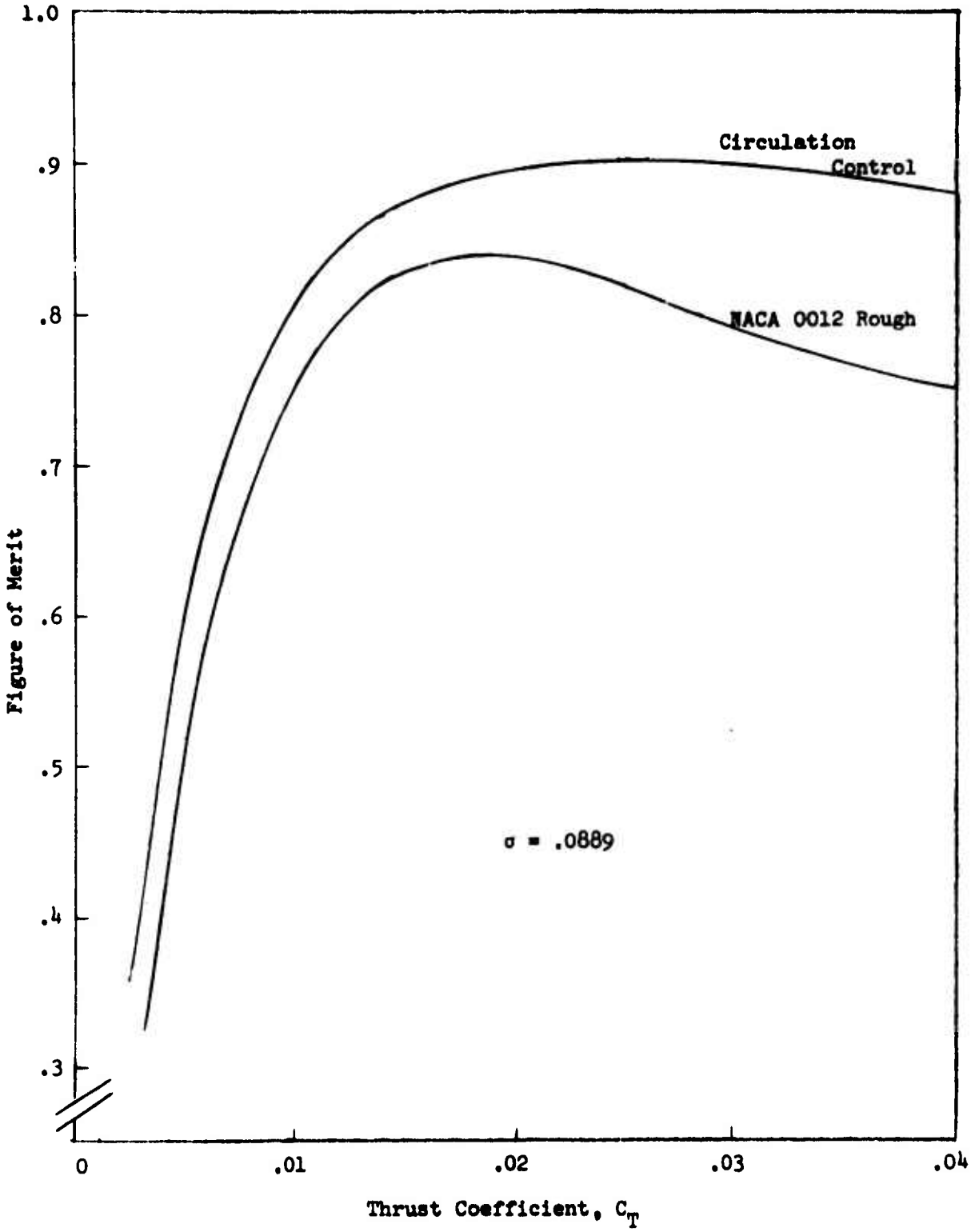

Figure 12 (Continued)
(c) C/R = .07

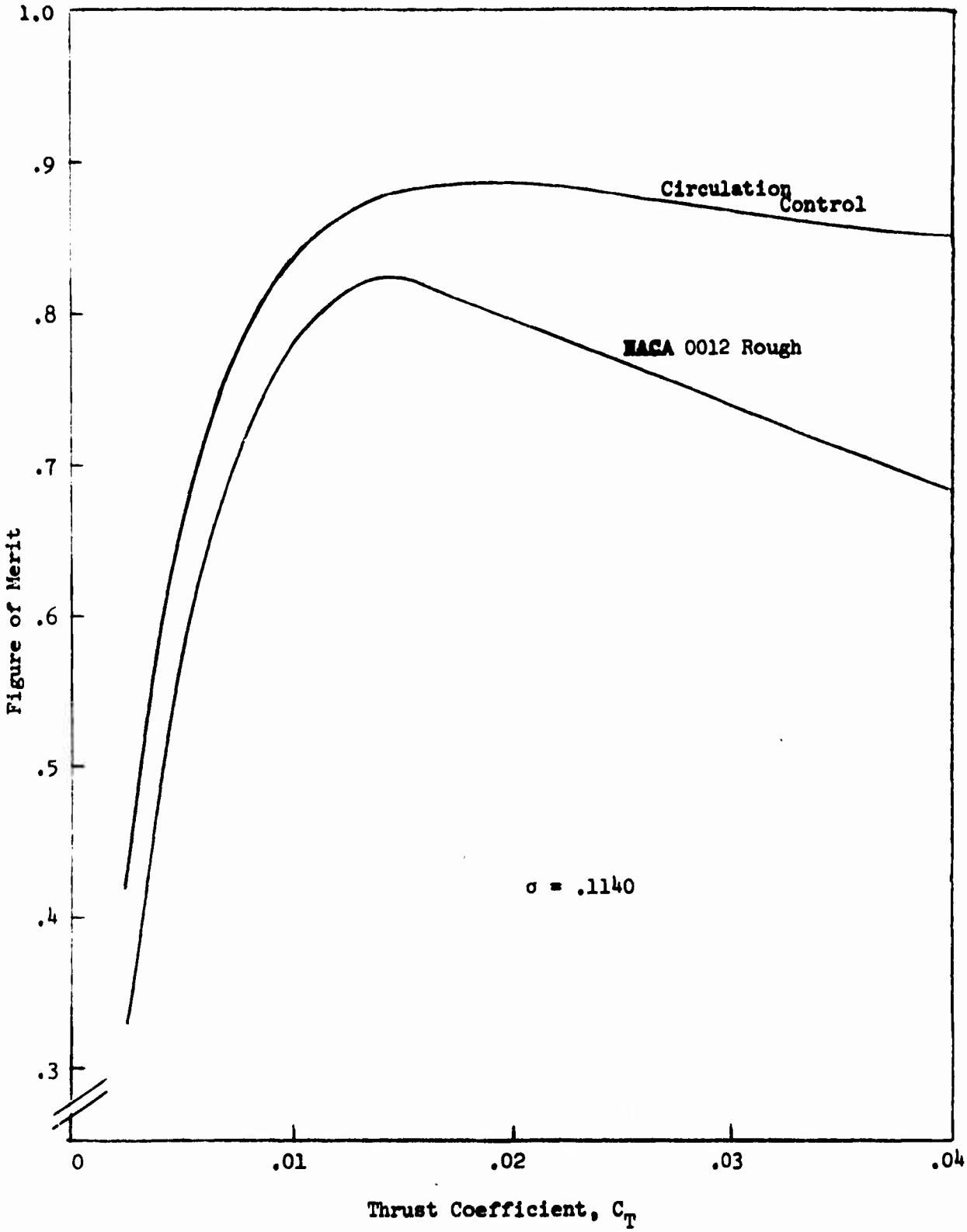

Figure 12 (Concluded)

(d) C/R = .09

Distribution
not shot

UNCLASSIFIED
Security Classification

DOCUMENT CONTROL DATA - R & D

(Security classification of title, body of abstract and indexing annotation must be entered when the overall report is classified)

1. ORIGINATING ACTIVITY (Corporate author)	2a. REPORT SECURITY CLASSIFICATION
Aviation & Surface Effects Department Naval Ship Research & Development Center Bethesda, Maryland 20034	UNCLASSIFIED
	2b. GROUP

3. REPORT TITLE

DETERMINATION OF THE (IDEAL PRACTICAL) HOVER EFFICIENCY OF CIRCULATION CONTROL ROTORS

4. DESCRIPTIVE NOTES (Type of report and inclusive dates)

Technical Note

5. AUTHOR(S) (First name, middle initial, last name)

Robert M. Williams and Rodney A. Hemmerly

6. REPORT DATE	7a. TOTAL NO. OF PAGES	7b. NO. OF REFS
August 1971	52	8

8a. CONTRACT OR GRANT NO.	9a. ORIGINATOR'S REPORT NUMBER(S)
b. PROJECT NO. RR011-05-04 WF32421.202	Technical Note AL-212
c.	9b. OTHER REPORT NO(S) (Any other numbers that may be assigned this report)
d. 690-011	

10. DISTRIBUTION STATEMENT Distribution limited to U.S. Government agencies only; Test and Evaluation; August 1971. Other requests for this document must be referred to Head, Aviation and Surface Effects Department (16).

11. SUPPLEMENTARY NOTES	12. SPONSORING MILITARY ACTIVITY
	Office of Naval Research ONR 460 Arlington, Virginia 22217

13. ABSTRACT

An approximate analysis of the maximum hover performance of a Circulation Control Rotor is presented. Closed form equations are developed which conveniently show the contribution of the induced, profile, compressor and coriolis powers in terms of the basic airfoil equivalent lift to drag ratios. A range of rotor taper ratios and solidities are examined under the constraint of ideal twist distribution. A comparison is made with a conventional rotor using a NACA 0012 reference airfoil. It is demonstrated that the circulation control rotor can achieve comparable overall hover efficiencies (Figure or Merit) at significantly higher values of rotor thrust coefficient to solidity ratio than conventional rotors. The implications of these characteristics for helicopter design is then discussed briefly.

DD FORM 1 NOV 68 1473 (PAGE 1)

UNCLASSIFIED
Security Classification

14 KEY WORDS	LINK A		LINK B		LINK C	
	ROLE	WT	ROLE	WT	ROLE	WT
Helicopter Rotor						
Jet Flap Rotor						
Circulation Control Rotor						
Boundary Layer Control						
Hover Performance						
High Lift Systems						